Point-by-point response to the reviews

The answers to the two referees is structured in the following way. We first address the comment from Referee 1, then the comments of Referee 2. In Grey are the comments of the referees and in black the answer we are providing and the modifications included in the text. At the end of the .pdf file, the word version including all corrections is added.

Point-by-point response to the first review

Comments from Referee 1: The paper presents the interpretation of landslide deposits from different sets of single-channel seismic reflection profiles across the Gulf of Corinth. From a hazard perspective, evidence of mass transport complexes is important, particularly if these can be linked to the preconditioning and triggering factors. In this area, recurrence rate of landslides appears significant, and as landslides can generate destructive tsunamis, assessing the source areas, causes and consequences are important. This is a well- written paper, with a good data set and logical structure, even though the content is largely descriptive. There are nevertheless a few points that I am missing from the paper:

Whereas identifying landslide deposits and obtaining the volumes involved are essential in a geohazard perspective, there is also a need to better define the land- slide processes and consequences.

- I am somewhat surprised to see that the source areas from the different landslide events remain very poorly constrained, despite the fact that some of the landslide deposits are quite large, and cover a significant part of the basin.

Author's response: Considering this question of the reviewer and some of the following ones, we realized that part of the context regarding the geohazard landslide perspective is missing.

First, we talk about earthquakes and landslides triggered by earthquakes, but did not provide a fault map. We presently add a new set of figures labeled Figure 1. At the top of Figure 1, we now display the active faults with the high resolution bathymetry obtained by Nomikou et al. (2011).

Second, another element was also missing. Readers without previous knowledge of the submarine context of the Gulf of Corinth would not realize that very large amount of uncompacted sediments are available in steep submarine delta slopes, which is a preconditioning factor. In the setting (line 70-74) we mention that "*the western gulf is bordered to the south by 400 m high Gilbert deltas built by the Erineos, Meganitis and Slinous river, and at its north-western end, by the fan delta of the Mornos River…. The delta fronts are highly unstable (..*". But the comments of the reviewer show that a more precise context is necessary.

Author's changes in manuscript: We now show in Figure 1 in addition to the active faults and the submarine bathymetry, which evidences the steep and wide delta fronts, the morphosedimentary map of Holocene deposits and the isopach maps of the Holocene and the previous glacial-interglacial period.

Author's response: The isopach maps evidence the very large volume of sediments accumulated on steep unstable slopes that is available for mass transport. Most landslide deposits documented in paper have sources in these steep overloaded delta fans located along the southern coast and at the north-western end of the Gulf. So in fact the source areas are broadly very well defined. However given that there are high quality multi-beam data available but only a high-resolution raster map of the bathymetry by Nomikou et al. (2011) it is not possible to define in more details the source areas.

Author's changes in manuscript: We change the setting section in the following way to provide clearer indication about the morphological setting and the inferred source areas located in steep slopes surrounding the flat basin. " *The western Gulf of Corinth is characterized by a relatively flat deep basin dipping gently to the east. Featuring a narrow canyon in the west, it widens in the east (Delphic Plateau, Fig. 1). It is bordered by steep slopes on all sides (Fig. 1) To the north, it is limited by the Trizonia scarp with slopes ranging from 25° to locally more than 35° and the associated Trizonia Fault (Nomikou et al., 2011); these slopes are mostly devoid of sediments which are trapped in the bay areas to the north (Fig. 1B). To the south, the western Gulf is bordered by 400m high Gilbert deltas built by the Erineos, Meganitis and Selinous rivers that lie in front of the active Psathopyrgos, Kamari and Aigion Faults running along or near the coastline. Delta fronts have 15° to 35° slopes incised by gullies (Lykousis et al., 2007; Nomikou et al, 2011) and consist of a thick pile of fine grained sediments. The delta-front sediments accumulated over the Holocene and the previous glacial-interglacial period have thicknesses, respectively, larger than 50m and 100 m (Fig. 1B and 1C; Beckers, 2015; Beckers et al, 2016). At the north-western end of the Gulf, lies the largest fan-delta of the Mornos River*

that drains 913 km2 and is by far the largest watershed among the rivers flowing toward the westernmost Gulf of Corinth (Fig. 1A). The delta fronts are highly unstable (Ferentinos et al, 1988; Lykousis et al., 2009), which favours frequent submarine landsliding (Stefatos et al., 2006; Tinti et al., 2007; Fig. 1B). During the last centuries, submarine landslides have been triggered by earthquakes and by sediment overloading on steep slopes (Galanopoulos et al., 1964; Heezen et al., 1966). Numerous debris-flow deposits and mass-transport deposits (MTDs) have thus accumulated at the foot of the deltas (Ferentinos et al., 1988; Beckers et al., 2016; Fig. 1B). Alongside these gravity-driven sedimentary processes, contour-parallel bottom-currents also influenced sediment transport in this area (Beckers et al., 2016).”

We also have clarified the section 5.2. Sediment sources in the following way: “*5.2 Sediment sources*

According to the mapping of the thickness of the deposits, large sliding events in the westernmost Gulf of Corinth mainly result from slope failures in, or close to, the Gilbert-type fan-deltas. Large sediment volumes were trapped in these deltas during the Holocene. As shown in Figure 1, Holocene foreset beds reach 40 to 60 m in thickness on average in the Eroneos and Meganitis fan-deltas, and sediment accumulation during the Holocene exceeding 100 m have been observed locally in between. These are the sources of MTD 10 in sliding event C and MTD 14 in sliding event D. The remarkable amount of sediments delivered to the gulf of Corinth during the Holocene probably results from large volumes of sediments stored onland during the last glacial period that were mobilized from river floodplains and colluvial deposits to rivers deltas. Widespread soil erosion resulting from human deforestation and agriculture during the second half of the Holocene also contributed to increase sediment fluxes in this period. Similarly, the previous period considered here spanning ~130 ka to ~11 ka is also characterized by a large sediment accummulation with a pile of 60 to 100 m forming the delta fronts of the Erineos and Meganitis delta (Fig. 1). These sources are one of the main source of MTD 10 in sliding event F.”

Comments from Referee 1 : The preconditioning and triggering factors remain uncertain. I note that the point (abstract) of dramatic changes in water depth and water circulation at 10-12 ka is only applicable to a some of the cases.

Author's response: The preconditioning and triggering factors are discussed at length in the paper with section 5.4 and 5.3. Some of the context about the preconditioning factors (i.e. quantity of sediments available on slopes for mass transport), and triggering factors (fault maps, and relation between fault map and sediment accumulation on slopes) was missing and is presently displayed in Figure 1. In addition we have clarified the section 5.2. Sediment sources (see above).

Comments from Referee 1 : Landslide dynamics and the tsunami potential are briefly mentioned but not really addressed. Such assessment would re- quire modelling, but also information about the soil properties, the source areas, etc. Not all landslides will create tsunamis (see Løvholt et al., 2017).

Author's response: We fully agree that assessment about landslide dynamics and tsunami potential is not fully addressed, because it is beyond the paper scope and would require modeling. In addition, it would require a precise knowledge of the landslide source area that we have not. We only have a first order estimate of most of the source areas (i.e. Erineos delta fan).

Comments from Referee 1 :The authors report landslide volumes, calculated from a (sparse) grid of seismic reflection profiles. The authors should mention the method used to obtain these values (e.g., gridding algo- rithm) as well as adding a statement about the uncertainty, particularly considering the line spacing of the seismic lines, and the lack of 3D seismic data. Can we be sure that the spatial extent mapped is a realistic impression of the failures or can they be over-estimated, due to the gridding and missing out areas where there are no deposits (but not evidenced because of the lack of data). This should be added as a key point under 5.1 Limitations of the analysis.

Author's response: We report landslide volumes and were extra careful in the mapping. The gridding algorithm was specified in the text: line 100-102 “an *inverse distance weighted interpolation between thickness data points was used to derive isopach maps of the deposits and estimate their total volume”.* For the small size MTD of SED A, the comparison with other volume evaluation shows that our volume evaluation is adequate. For MTD with a large size, the volume would be adequate because of the large surface area sampled by numerous seismic profiles. We are uploading Figure 2 that show the mapping of the MTDs with the seismic grid, but we are not considering to include the seismic grid in the published version of figure 2 because it would be difficult to read it with the grid.

Author's changes in manuscript: We would include the seismic grid in the figure 7 showing the largest MTDs (MTD 10, MTD 14 and MTD 17). The figure 7 uploaded thus now shows the seismic grid and the inferred mapping that took into

account the geomorphological and topographical constraints: MTD10, 14 and 19 to the north were constraints by the Trizonia scarp.

Author's response: Two versions of Figure 2 were uploaded: one as we want to include it the paper and the other with the seismic grid in response to the reviewer comment. We prefer to indicate the seismic grid in Figure 7 and not in Figure 2, because it was more difficult to read figure 2 with the grid.

Comments from Referee 1: What is the onshore-offshore relationship of the landslides?

Author's response: There is a priori no relationship. All submarine landslides originate from the submarine delta-fans. Landsliding is documented onshore on the northern coast and along the Psathopyrgos scarps, but it has no influence on the submarine landslides documented. The new figures 1 added now provide the necessary context for a better understanding to readers

Comments from Referee 1: In the interpretation, the authors repeatedly refer to blanking but they do not really illustrate what is it and what the causes may be.

Author's response: We agree with the reviewer that we do not illustrate what is it and what the causes may be. So we add some more details and differentiate more clearly in the text the different blanking areas and stratigraphy that have unclear origin. First, blanking occurs below the Holocene and in two distinct spots. In the Mornos Canyon, a wide blanking area exists at a depth of about 50 to 70 m below the sea floor, a few meters below reflector 1, in direct continuity with the fan delta of the Mornos River. The origin of the blanking is unknown, but it is a low-stand related feature related to the Mornos Delta and it might correspond to coarse grained, organic rich sediments. Another area with blanking occurs at the junction between the Mornos Canyon and the Delphic plateau at the foot of the Erineos foreset beds, at a depth similar to SE F (MTD 19); it is associated with strongly disturbed sediments forming mounds. Its origin is unknown, but it might be related to a MTD. Finally there are uncertainties regarding the southward extension of MTD 14. It extends into a zone of chaotic reflections and very disturbed seismic stratigraphy of unclear origin. Our estimate of the volume of MTD 14 was thus conservative and is considered as a minimum.

Author's changes in manuscript: To clarify the statements, we have rewritten the paragraph line 199- 207 dealing with the blanking and uncertain area in the following way. "*In some zones (Fig. 2), the existence or the geometry of MTDs is difficult to evaluate because of seismic blanking and strong chaotic reflections affecting some stratigraphic intervals. Above reflector 1, the stratigraphy is clear except regarding the southern extension of MTD 14 in SE D. The low amplitude, almost transparent reflections characterizing the MTD deposit extends until a more chaotic and thicker deposit associated with surface mounds (Fig. 5). We could not decipher if the chaotic reflections that disturb the seismic stratigraphy was associated with MTD 14 in SE D or in relation with sediment remobilization from the underlying sliding event F (Fig. 4). So the mapped extension of MTD 14 in Fig. 2E is conservative and considered as a minimum. Below reflector 1, the amplitude of the reflectivity sharply decreases, which is a characteristic of lowstand deposits in the Gulf (Bell et al., 2008), and blanking occurs in two areas .In the Canyon area, a wide blanking area exists at a depth of about 50 to 70 m below the sea floor, a few meters below reflector 1, in direct continuity with the delta of the Mornos River. Blanking is thus a low-stand related feature and might correspond to coarse grained, organic rich sediments of the Mornos River. Consequently, the stratigraphy of MTDs between reflectors 2 and 1 is well established only below the Delphic Plateau. The other area associating with blanking and strongly disturbed sediments forming mounds occurs at the junction between the Canyon and the Delphic plateau at the foot of the Erineos foreset beds, at a depth similar to SE F. Its origin is unknown, but it might be related to an MTD deposit in relation with MTD 19."*

Comments from Referee 1: Likewise, the authors refer to coarser grained material in a deformed mass transport deposit, but there is no evidence for this. I doubt that one would be able to observe this from sparker data, as the masses are essentially deformed. Maybe speculation?

Author's response: We evidenced that the MTD are usually lenticular bodies of low-amplitude, incoherent reflections.
Author's changes in manuscript: We removed the sentence referring to coarse-grained deposits line 140: "*which would make them different from the coarse-grained deltaic deposits that are known to fail relatively frequently along the southern coast.*" The text is now explicit about the limit of the interpretation of the MTD facies: "*In the Delphic Plateau basin (eastern part of the deep flat basin), most MTDs are imaged as lenticular bodies of low-amplitude, incoherent reflections (Fig. 3 and 4). They generally have a flat upper surface and pinch out on their margins. Their thickness ranges between a few meters, which is the minimal thickness for a MTD to be imaged with the seismic system used, and 53 meters. The geometry and seismic facies indicate subaquatic mass-flow deposits (e.g. Moernaut et al., 2011, Strasser et al., 2013). The seismic facies of many MTDs also suggests a fine-grained lithology. However, this statement must be viewed cautiously considering the uncertainties on the interpretation of seismic facies in terms of grain-size, especially for reworked sediments. For instance, failure of coarse-grained*

deltaic deposits commonly result to their total disaggregation and transformation into grain flows and turbidity currents, whereas finer grained deposits evolve as landslides and cohesive debris flows (Tripsanas et al., 2008)."

Author's response: But in the next paragraph (line 145-149), we still want to evidence that some MTD display a different facies with high-amplitude reflections and coherent layering, which could be related to coarse-grained sediments.

Author's changes in manuscript: We change the sentence, to evidence that it was a possible interpretation: "*In the Canyon basin (western part of the deep flat basin), the MTDs present the same general characteristics but the reflector pattern is more variable (Fig. 4). Some high-amplitude reflections* ***and coherent layering*** *are observed in some MTDs,* ~~*revealing*~~ *suggesting coarser-grained sediments and locally preserved* ***stratigraphy****."*

Author's response: So in the section 5.2. Sediment sources, we are discussing the observation about the two types of seismic facies observed regarding the MTD. We are also providing more information about the fact that the foresets are made of a thick accumulation of stratified fine-grained sediments and that are not made of coarse grained sediments.
Author's changes in manuscript: The text as been corrected as followed: "***The*** *seismic facies of most large MTDs* ***also*** *implies that they are likely composed mainly of fine-grained sediments****, and*** ***s****eismic profiles* ***across*** *fan-delta area have shown that the pro-delta foresets are locally made of a thick accumulation of stratified fine-grained sediments .* ***These fan-delta sediments*** *are probably the main source of sediments for the largest MTDs (MTD 10, 14 and 19). However, some smaller MTDs seem to be made of coarser-grained sediments according to the seismic character (e.g., in SEs A and B in the Canyon basin), suggesting failure also occurred in coarser-grained parts of the fan-deltas located* ***at the junction between the topset and the foreset*** *(e.g., the 1963 slide in the Erineos fan-delta)."*

Comments from Referee 1: Smaller comments:

I would recommend making the seismic profiles with the same vertical exaggerations or same scales to facilitate comparison. Likewise, please add an indication on the figures where the seismic lines cross.

Author's response: We purposely chose to show the seismic profile with different vertical exaggerations, in order to be able to evidence the different features we wanted to illustrate.

We purposely chose not used the same scale or vertical exaggeration for all seismic profiles because our goal is to illustrate deposits and structures that have very different sizes, from 1 to ~10 km in length and from ~4 to ~40 m in thickness. If we choose the same vertical scale for all profiles, small-scale evidences will not be visible.

Comments from Referee 1: Terminology is in places confusing. I understand from this paper that landslide event actually refers to a certain interval in time (not specified) during which various landslides (with different source locations) may occur. Thus, different landslides compose a landslide event.

Author's response: Yes your understanding is correct, but because the terminology was confusing we choose to further clarify our statements.

Author's changes in manuscript: We change the related paragraphs: *The stratigraphic position of MTDs in the Canyon and in the Delphic Plateau basins is not random. Most of them are* ***clustered and are defining*** *multi-MTDs temporal "events", based on* ***common*** *un-deformed underlying or overlying reflections that can be followed across the basin. Such correlations suggest that six* ***clustered*** *events of large submarine mass wasting occurred over the last 130 ka. Two sliding events (SE) are represented by* ***clustered*** *MTDs located between reflectors 2 and 1 (SE E and F). The four others occurred during the Holocene: SE D comprises MTDs deposited just on top of the reflector 1, SE C is located in the middle of the Holocene sequence, SE B somewhat higher, and finally SE A includes MTDs that outcrop at the sea floor.*

....

The definition of sliding events ***reflects a clustering of submarine landslides in a relatively short period of time****.* ***It*** *does not necessarily imply a synchronous occurrence of all submarine landslides included in one event. Indeed, the accuracy of the correlation between separated MTDs that are interpreted to belong to the same sliding event is in the order of one or two reflections in the seismic data.* ***Deciphering the exact MTD chronology within a sliding event was not possible because*** *of the discontinuous character of many reflections and the relatively large distance that separates some MTDs (up to 8.5 km). This "stratigraphical" uncertainty corresponds to ~1-2 meters of sediment so, based on sedimentation rate estimates, sliding events represent a set of MTDs that* ***occurred over a period of 300 to 1000 years*** *(Lykousis et al., 2007).*

Comments from Referee 1 :The map should contain all geographical references used in the text. This is currently not the C2 case.

Author's response: Geographical references have been added to the new figure 1.

Comments from Referee 1 :On Figure 1, I would recommend adding a colour-coded (shaded relief or so) topographic/bathymetry map and slope map, as both are important to understand the processes. The maps should ideally cover the onshore and offshore part. Note that the "grey lines" referred to are not only the seismic grid but also bathymetric contour lines. Add the location of the Delphic Plateau, and the "Canyon".

Author's response: A new Figure 1 has been added to provide needed context taking into account remarks from the reviewer; a shaded topography was also added. The old figure 1 is now figure 2.

Author's changes in manuscript: New Figure 1 taking into account the remarks of referee 1.

Comments from Referee 1 : There are a few typos in the text - Figure 2: explain the horizons [1] and [2].

Author's response: We explain them.
Author's changes in manuscript: In the caption of figure 2, we now state: "*Figure 2. E-W Sparker seismic profile showing the mass transport deposits imaged in the Delphic Plateau basin. See the location of the profile in Fig. 1. Horizon [1] indicates the beginning of the last post-glacial transgression, at 10.5-12.5 ka and horizon [2] the marine isotopic stage 6 to 5 transgression, which occurred at ca. 130 ka (Cotterill, 2006; Beckers et al., 2015; 2016)"*

Comments from Referee 1: The term "outcrop" suggests that something was eroded on top. This may not be the case for the youngest landslide deposits. Consider using exposed as the seafloor

Author's response: We took into account this comment.

Author's changes in manuscript: line 197-198: *SE A includes MTDs that outcrop at the sea floor* was change to ***SE A includes MTDS at or near the seafloor responsible for the present-day hummocky topography of the seafloor***

line 219: *Sliding event A: Eight MTDs that outcrop at the sea floor have been identified.* was changed to ***Sliding event A: Eight MTDs at or near the seafloor have been identified.***

Comments from Referee 1 : Figure 6 is too small, and ideally, the maps should all use the same area, to facilitate comparison. This would be a good place to add the various source areas.

Author's response: We took into account this comment.

Author's changes in manuscript: We enlarge Figure 6 and use the same area to facilitate comparison. We also place the different source areas.

Point-by-point response to the secoond review

Comments of referee 2:
Overview The paper describes the frequency and characteristics of small volume submarine landslides in the Gulf of Corinth over the past 130 ka. The landslides have the potential to generate hazardous tsunamis, with one historical event recorded. Potential landslide preconditioning and triggers are discussed. Six major landsliding events are recognised, of which three are relatively large volume. The age of the events are dated by their relationship to two regional seismic horizons interpreted as major flooding events and dated at 130 and 10-13ka. Most slide events (four) are identified as Holocene, with two others older than 10 to 12 ka. Although the volumes of most slides are quite small (largest 1km3) one,

in historical times (1995), generated a significant tsunami.
Author's response: Note that there was another significant tsunami generated during historical times by one of the slide we have mapped: the 1963 tsunami was generated by a submarine landslide on the Erineos prodelta. Moreover, numerous other historical tsunamis have been reported in the western Gulf of Corinth: 1996, 1984, 1965, 1888, 1887, 1861, 1817, etc. (the full list is in Papadopoulos, 2003, Natural Hazard; summary in Beckers et al., 2017, Marine Geology)

Comments of referee 2: The paper is a dense read, because of the number and complexity of the landslide failures and the relationships to triggering mechanisms and preconditioning.

Comments of referee 2: The strengths of the paper are in the seismic data and its interpretation. The weakness is the lack of sample data to identify the sedimentology of the slides and their ages, which are based on the slides relationships to the two regional horizons. As with all submarine landslides, earthquakes are proposed as the most likely trigger. Earthquake records (from sediments) are confined to the past 17 thousand years, with frequencies of 400-500 years for the period 12-17ka in the central Gulf of Corinth and in the western Gulf (from palaeoseismology) 200 to 600 years. Preconditioning factors are identified from events in other regions outside the western Gulf.

Author's response: We fully agree with the referee about the paper weakness. There are no long coring across the western gulf of Corinth, to establish a relationship between MTDs, their sedimentological imprint and an earthquake catalogue.

Comments of referee 2: Focussing on the science, I am surprised that the dated regional horizons are not used more fully to understand sedimentation rates and the potential rates of sediment recharging in the western basin. These might better inform on the local differences between the glacial and post glacial environments that would influence slide failure.

Author's response: We have now added new data in figure 1 showing isopach 1 of the Holocene and of the previous glacial interglacial period in answer to referee 1, but we have not fully exploited the data to discuss the potential influence of sediment recharging in the western basin. In the discussion, we now stress that there is a large difference regarding the sediment recharging between the Holocene Period and the previous 130-12kyrs one.
Considering the spot between the Erineos and the Meganitis delta-fans (See Fig. 1) where we could have a reliable record of sediment accumulation over the last 130 kyrs, up to ~ 100 m were accumulated over the last 10.5 to 12.5 kyrs and up to 125 m were accumulated over the previous ~120 kyrs period. So there is an order of magnitude difference in sediment recharging between the Holocene and the previous period. We are now discussing these facts in the text.

Author's changes in manuscript:
Change in the Discussion section
5.5 Other potential triggers and pre-conditioning factors

...Overall, these data suggest that the Last Glacial probably experienced the largest sedimentation rates over the last 130 ka in most of the Gulf of Corinth. This inference is however not valid at the western tip of the Gulf. The comparison between isopach maps of the Holocene and the anterior 130-12 kyrs period evidences a large Holocene increase in sedimentation accumulation rate (Fig. 1). In the Delphic plateau basin, average sedimentation rate (excluding the thickness of MTDs) reaches ~2.4 mm/yr for the Holocene and ~ 0.4 mm/yr for the previous 120 kyrs. This is in line with the fact that only one large sliding event F was recorded during the ~60 ky-long Last Glacial. Increased sedimentation is thus a pre-conditioning factor of landsliding in the western Gulf.

Comments of referee 2:
I am also surprised that there is not more consideration of the major difference between the glacial and Post glacial sea levels in the context of the slides and their headscarps. Consideration of Figure 1 suggests that lowering sea level by 60 metres makes a major difference in some regions that may influence sedimentation and sliding. Whether the difference in sea levels is important or not, it would be informative to see the effects on a figure.

Author's response: We agree that the lowering sea level might make a difference in some part of the Gulf but not a major one regarding the delta-front bordering the southern edge of the western Corinth Gulf. The new figure 1 showing the high resolution bathymetry of Nomikou et al. (2011) clearly show that the isobaths -100 is located close to the shoreline all along the faulted southern coast west of Aigio, and that the foreset beds extend to isobaths -300m. So the

submarine slopes where submarine landslides can initiate are not significantly different between the Last Glacial Period and the postglacial period, they might be a little more restricted during the Last Glacial Period.

Author's changes in manuscript:
The following clarification was included in the Discussion section and the subsection 5.5 Other potential triggers and pre-conditioning factors

…
During this lowstand period, the extent of submarine slopes where submarine landslides can initiate were not significantly reduced, because the foreset beds of the Erineos and Meganitis that are the largest source of mass wasting sediments for the Delphic plateau extend down to the ~300 m isobaths. The steepest slopes of these two prodeltas are located above isobaths -100m and between isobaths -150m and -200m according to the slope map of Nomikou et al. (2011), so unstable slopes above -60m that were submerged only in the postglacial period cover a restricted area. …

Comments of referee 2:
It would also help the reader if some of locations of data which underpin the interpretations, which are outside the area were identified on a map. These include the Philious Basin (Page 13, lines 457-458) and the Alkyonides basin (Page 113, Line 467).
Identifying the location of these would identify their relevance.

Author's response:
We fully agree with the reviewer that the reader needs to know were the locations of data, which underpin the interpretations need to be added. However the paper is already long with 9 figures and we did not want to include a new one. So we choose to indicate clearly in the text the relevant information regarding the location of the data with respect to the Gulf of Corinth.

Author's changes in manuscript: in the Discussion section and the subsection 5.5 Other potential triggers and pre-conditioning factors
Regarding the location of the Alkyonides Basin, we add the clarification that it is located at the eastern tip of the Gulf in the following way: "*Collier et al. (2000) suggest that the denudation rate at the eastern end of the Gulf in the Alkyonides Basin"*
Regarding the location of the Philious Basin we did the same: "Fuchs (2007) presents the evolution of sedimentation rates in colluvial deposits on the southern shoulder of the Corinth Rift, in the Philious Basin, …"

Comments of referee 2:
The interpretation of the earthquake triggering of the landslides is undoubtedly reasonable, but the evidence is very sparse. It seems that only the 1995 earthquake triggered the MTD at the foot of the Meganitis fan, but this is hypothetical. What was the trigger of the 1963 landslide which caused a major tsunami, was it just sediment loading? The following discussion of the relationships between earthquake frequency and landsliding is also question able, because it is assumed that the earthquake frequency for the glacial period is the same as for the Holocene (page 12, lines 416-418) which seems to me to be unlikely.
This is quite a jump in the interpretation as it underpins much of the subsequent discussion on triggering and preconditioning – but that is always the problem with MTDs. I guess it doesn't invalidate the interpretations too much.

Author's response: There are no relationship between the earthquake frequency and climatic changes. The earthquake cycle is linked to loading on faults due to geodynamic processes at depth independent of surface processes. So indeed we assumed that earthquake frequency is nearly constant. There are still some potential effects on the seismicity due to the rapid water level changes at the beginning of the Holocene, which would have change the stress field and the pore pressure. But nobody has modeled it, and its effects on the fault system in the Gulf of Corinth are unknown. Any lenghly discussion about it would be very speculative. We still include a short sentence to take into account the referee remark.

Author's changes in manuscript: in the Discussion section and the subsection 5.5 Other potential triggers and pre-conditioning factors

"The deposition of SE D occurred at 10-12 ka, when the water level started to increase in the Corinth Gulf. Water level change might change the stress field and pore pressure potentially affecting the earthquake cycle. Water level increase and bottom current initiation would also.."

Author's response:

The earthquake frequency might also have changed because of change in the geodynamics of the rift over the 130 kyrs timescale. Previous studies (i.e. Ford, M., et al. "Rift migration and lateral propagation: evolution of normal faults and sediment-routing systems of the western Corinth rift (Greece)." Geological Society, London, Special Publications 439.1 (2017): 131-168) suggest a rapid evolution with respect to fault growth and linkage. Demoulin et al. (2015) also evidenced an Holocene acceleration of the strain rates using fluvial morphometry and we also found a large increase in Holocene subsidence rate compared to the previous period probably linked with an acceleration of the deformation (Beckers, A., 2015, Late quaternary sedimentation in the western gulf of Corinth: interplay between tectonic deformation, seismicity, and eustatic changes, PhD thesis, pp. 260), but these later finding will be independently published in a peer-review journal. Given the uncertainties about the earthquake frequency, we choose not to have an extended discussion about the topics, because it would be too speculative. We still have included the following changes in the text

Author's changes in manuscript : in the Discussion section and the subsection *5.4. The possible role of large earthquakes*

"This high Holocene frequency compared with the ~120 kyrs anterior period may be attributed to two factors. First it might be a bias, because the seismic reflections corresponding to the last glacial period (110-12ka) are less clear (lower amplitude and lower continuity) than the reflections from the Holocene interval. Consequently, medium-sized landslides such as those detected in SEs A and B might have been missed in the seismic unit between reflectors 2 and 1. Second, it could be attributed to a change in earthquake frequency due to a Holocene acceleration of the strain rates that was evidenced by fluvial morphometry (Demoulin et al., 2015) and subsidence markers (Beckers, 2015)."

Comments of referee 2:

Regarding my comment on the complexity of the paper, I make some suggestions. There are geographical names mentioned in the text, which are not on the figures, e.g, Delphic Plateau, Canyon basin, possibly others.

Author's response: We made modifications to mention the names in the figures already for referee 1.

Comments of referee 2:

With regard to the organisation of the paper, I found it hard to understand the full setting of the GoC from the background sections because back ground material is distributed later in the paper.
Other material which should be presented early on in the Background includes; the stratigraphic framework (Page 2 lines 90-95) and the palaeolake levels (Page 13 lines 477-485). Including these would provide a broader picture to background the environmental changes over the 130 ka time period.

Author's response : We already change the setting section to provide a clearer picture according to the remarks of referee 1, but we now include a new paragraph in the setting to provide more information also regarding the stratigraphic framework and the palaeolake levels.

Author's changes in manuscript :

The following paragraph was added to the setting section:

The shallow sedimentary infill of Gulf of Corinth infill consists of a distinct alternation between seismic-stratigraphic units with parallel, continuous high-amplitude reflections and units with parallel, continuous low amplitude reflections to acoustically transparent seismic facies (e.g. Bell et al., 2008; Taylor et al., 2011). Generally, the semi-transparent units are thicker than the highly reflective units (e.g. Taylor et al., 2011). These alternating seismic-stratigraphic units have been observed throughout the Gulf of Corinth and have been interpreted as depositional sequences linked to glacio-eustatic cycles (Bell et al., 2008; Taylor et al., 2011). Because of the presence of the 62 m deep Rion Sill at the entrance of the Gulf, the Gulf of Corinth was disconnected from the World Ocean during Quaternary lowstands and was thus a non-marine sedimentary environment. The marine and non-marine environments are associated with different climatic regimes (e.g. Leeder et al., 1998). During glacial stages, the sparse vegetation cover was more favourable to erosion than during interglacials, so high quantities of sediments were routed towards the Gulf (Collier et al., 2000). These lowstand deposits appear as thick, low-reflective units. The thin, high-reflective units are interpreted to represent the marine highstand deposits. The last lacustrine-marine transition has been sampled in different sedimentary cores (Collier et al., 2000; Moretti et al., 2004; Van Welden, 2007; Campos et al., 2013).

Conclusions Apart from my above comments, this is an interesting paper identifying the potential hazard from submarine landslides in an enclosed basinal area, where future events, if of sufficient volume would be a tsunami hazard. It is well organized and well written. The remote data set is good, the temporal controls on the events are weak, but the innovative approach, using the (sparse) data applicable to this, results in a plausible story which should be published with some modification.

CHARACTERISTICS AND FREQUENCY OF LARGE SUBMARINE LANDSLIDES AT THE WESTERN TIP OF THE GULF OF CORINTH

Arnaud Beckers1,2*, Aurelia Hubert-Ferrari1, Christian Beck2, George Papatheodorou3, Marc de Batist4, Dimitris Sakellariou5, Efthymios Tripsanas6, Alain Demoulin1

1 Department of Geography, University of Liège, allée du 6 août 2, 4000 Liège, Belgium. Email : beckersarnaud@gmail.com.
2 ISTerre, CNRS UMR 5275, University of Savoie, F-73376 Le Bourget du Lac, France.
3 Department of Geology, University of Patras, Greece
4 Department of Geology and Soil Science, Gent
5 Institute of Oceanography, Hellenic Center for Marine Research, GR-19013 Anavyssos, Greece
6 Gnosis Geosciences, Edinburgh, EH10 5JN, U.K.

* Now at: CSD Engineers, Namur Office Park 2, Avenue des dessus de Lives, 5101 Namur, Belgium

Correspondence to: Aurelia Hubert-Ferrari (aurelia.ferrari@ulg.ac.be)

Abstract

Coastal and submarine landslides are frequent at the western tip of the Gulf of Corinth, where small to medium failure events (10^6-10^7 m^3) occur on average every 30-50 years. These landslides trigger tsunamis, and consequently represent a significant hazard. We use here a dense grid of high-resolution seismic profiles to realize an inventory of the large mass transport deposits (MTDs) that result from these submarine landslides. Six large mass wasting events are identified, and their associated deposits locally represent 30% of the sedimentation since 130ka in the main western Basin. In the case of a large MTD of ~1 km^3 volume, the simultaneous occurrence of different slope failures is inferred and suggests an earthquake triggering. However, the overall temporal distribution of MTDs would result from the time-dependent evolution of pre-conditioning factors, rather than from the recurrence of external triggers. Two likely main pre-conditioning factors are (1) the reloading time of slopes, which varied with the sedimentation rate, and (2) dramatic changes in water depth and water circulation that occurred 10-12ka ago during the last post-glacial transgression. Such sliding events likely generated large tsunami waves in the whole Gulf of Corinth, possibly larger than those reported in historical sources considering the observed volume of the MTDs.

1 Introduction

The study of marine geohazards through their imprint in the late Quaternary sedimentary record is of great significance, since it can provide further information on geohazard events recorded in historical records, or even extend this record to much earlier times. The identification and recurrence patterns of mass transport deposits (MTDs) resulting from submarine landslides in sedimentary basins and lakes provide valuable information on possibly associated tsunamis as well as their potential trigger (e.g. earthquake). Tsunami hazard is particularly an issue of concern in the Mediterranean Sea where more than 300 tsunamis have been listed in the historical and sedimentary records (Soloviev, 1990; Salamon et al., 2007; Lorito et al., 2008).

This paper focuses on the Gulf of Corinth, Greece, located in the most seismically active part of the Corinth Rift. This area shows one of the largest seismic hazard in Europe (Woessner et al., 2013) and is affected by a tsunami once every 19 years on average, leading to a significant risk (Papadopoulos, 2003; Papathoma and Dominey-Howes, 2003). The gulf's western tip is the most active part of the Corinth rift, characterized by an extension of 15 $mm.yr^{-1}$ (Briole et al., 2000), and by frequent submarine or coastal landslides (e.g. Henzen et al., 1966; Papatheodorou and Ferentinos, 1997; Lykousis et al., 2009). Small to medium failure events (10^6-10^7 m^3) occur on average every 30-50 years (Lykousis et al., 2007a). These landslides trigger tsunamis (Galanopoulos et al., 1964; Stefatos et al., 2006; Tinti et al., 2007) and induce coastal erosion by upslope retrogression (Papatheodorou and Ferentinos, 1997, Hasiotis et al., 2006). Tsunamis reaching an intensity ≥ 4 consequently represent a significant hazard in the western Gulf of Corinth (Beckers et al. 2017), and are documented for the last two millennia from historical

sources and onland geological studies (De Martini et al., 2007; Kontopoulos and Avamidis, 2003; Kortekaas et al., 2011). However, these data sets are incomplete.

A dense grid of high-resolution seismic profiles acquired in this area (Beckers et al., 2015) was used to realize an inventory of the large mass transport deposits (MTDs) that may be interpreted as the result of submarine landslides. Dated from the Late Pleistocene and the Holocene, the mapped mass transport deposits range from 10^6-10^9 m^3. Average recurrence intervals are presented and discussed, as well as pre-conditioning factors that might have played a role in the occurrence of these large submarine landslides. The MTDs' temporal distribution is discussed, as well as the implications of their occurrence on tsunami hazard.

2 Setting

The western Gulf of Corinth is characterized by a relatively flat deep basin dipping gently to the east. Featuring a narrow canyon in the west (the Mornos Canyon), it widens in the east (Delphic Plateau, Fig. 1). It is bordered by steep slopes on all sides (Fig. 1) To the north, it is limited by the Trizonia scarp with slopes ranging from 25° to locally more than 35° and the associated Trizonia Fault (Nomikou et al., 2011); these slopes are mostly devoid of sediments which are trapped in the bay areas to the north (Fig. 1B). To the south, the western Gulf is bordered by 400m high Gilbert deltas built by the Erineos, Meganitis and Selinous rivers that lie in front of the active Psathopyrgos, Kamari and Aigion Faults running along or near the coastline. Delta fronts have 15° to 35° slopes incised by gullies (Lykousis et al., 2007; Nomikou et al, 2011) and consist of a thick pile of fine grained sediments. The delta-front sediments accumulated over the Holocene and the previous glacial-interglacial period have thicknesses, respectively, larger than 50m and 100 m (Fig. 1B and 1C; Beckers, 2015; Beckers et al, 2016). At the north-western end of the Gulf, lies the largest fan-delta of the Mornos River that drains 913 km^2 and is by far the largest watershed among the rivers flowing toward the westernmost Gulf of Corinth (Fig. 1A). The delta fronts are highly unstable (Ferentinos et al, 1988; Lykousis et al., 2009), which favours frequent submarine landsliding (Stefatos et al., 2006; Tinti et al., 2007; Fig. 1B). During the last centuries, submarine landslides have been triggered by earthquakes and by sediment overloading on steep slopes (Galanopoulos et al., 1964; Heezen et al., 1966). Numerous debris-flow deposits and mass-transport deposits (MTDs) have thus accumulated at the foot of the deltas (Ferentinos et al., 1988; Beckers et al., 2016; Fig. 1B). Alongside these gravity-driven sedimentary processes, contour-parallel bottom-currents also influenced sediment transport in this area (Beckers et al., 2016).

The shallow sedimentary infill of Gulf of Corinth infill consists of a distinct alternation between seismic-stratigraphic units with parallel, continuous high-amplitude reflections and units with parallel, continuous low amplitude reflections to acoustically transparent seismic facies (e.g. Bell et al., 2008; Taylor et al., 2011). Generally, the semi-transparent units are thicker than the highly reflective units (e.g. Taylor et al., 2011). These alternating seismic-stratigraphic units have been observed throughout the Gulf of Corinth and have been interpreted as depositional sequences linked to glacio-eustatic cycles (Bell et al., 2008; Taylor et al., 2011). Because of the presence of the 62 m deep Rion Sill at the entrance of the Gulf, the Gulf of Corinth was disconnected from the World Ocean during Quaternary lowstands and was thus a non-marine sedimentary environment. The marine and non-marine environments are associated with different climatic regimes (e.g. Leeder et al., 1998). During glacial stages, the sparse vegetation cover was more favourable to erosion than during interglacials, so high quantities of sediments were routed towards the Gulf (Collier et al., 2000). These lowstand deposits appear as thick, low-reflective units. The thin, high-reflective units are interpreted to represent the marine highstand deposits. The last lacustrine-marine transition has been sampled in different sedimentary cores (Collier et al., 2000; Moretti et al., 2004; Van Welden, 2007; Campos et al., 2013).

3 Data and Method

Two seismic reflection surveys were carried out in 2011 and 2014 with the aim of imaging the subsurface below the westernmost Gulf of Corinth floor. The data were acquired by the Renard Center of Marine Geology of the University of Ghent along a grid of 600 km high-resolution seismic profiles

Aurélia Ferrari 7/2/2018 15:01
Deleted: It

Aurélia Ferrari 7/2/2018 15:01
Deleted: to the south

Aurélia Ferrari 7/2/2018 15:02
Deleted: and, a

Aurélia Ferrari 7/2/2018 15:02
Deleted: its

Aurélia Ferrari 7/2/2018 15:03
Deleted: by

Aurélia Ferrari 7/2/2018 15:04
Deleted: but some also occurred because of

Aurélia Ferrari 7/2/2018 15:04
Deleted: see also a facies map in

Aurélia Ferrari 21/3/2018 16:36
Formatted: Normal, No widow/orphan control, Don't adjust space between Latin and Asian text, Don't adjust space between Asian text and numbers

Aurélia Ferrari 21/3/2018 16:36
Formatted: Font color: Black, French

with a "CENTIPEDE" Sparker seismic source combined with a single-channel high-resolution streamer as receiver (see details in Beckers et al., 2015, the seismic grid is shown in Fig. 2). The expected vertical resolution at depth is ~1 m. In the deep basin (Canyon and Delphic Plateau areas, Fig. 1), the maximum penetration depth below the sea floor is about 360 ms TWTT (two-way travel time) to the east and about 100 ms TWTT to the west, i.e., 270-360 m and 75-100 m, respectively.

The inferred stratigraphic framework (Beckers et al., 2015) permits to identify two temporal horizons. Reflector 1 has been mapped in the whole study area, except in a basin west of the Trizonia Island (Fig. 1). This reflector corresponds to the beginning of the last post-glacial transgression, at 10.5-12.5 ka (Cotterill, 2006; Beckers et al., 2016). The second temporal horizon, 'reflector 2', has been mapped in the Delphic Plateau area only. It corresponds to the marine isotopic stage 6 to 5 transgression, which occurred at ca. 130 ka.

Aurélia Ferrari 13/2/2018 10:52
Deleted: 1

Figure 1. Study area with at the top, the fault map of Beckers et al. (2015) with the bathymetry from Nomikou et al. (2011), in the middle, the morphosedimentary map of Holocene deposits of Beckers et al. (2016), at the bottom the isopach maps of the Holocene (Right ; Beckers et al., 2016), and of the preceding period from 10 to 130 ka (Left ; Beckers, 2015). White areas in the bottom figures correspond to the ones with poor data or with an absence of stratigraphic marker. Grey curves in middle and bottom figures are sea floor contour lines interpolated from the seismic grid.

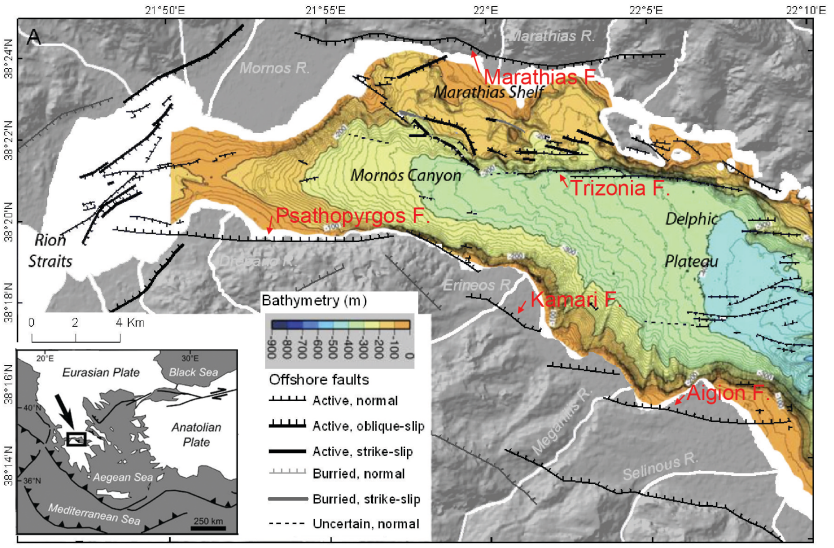

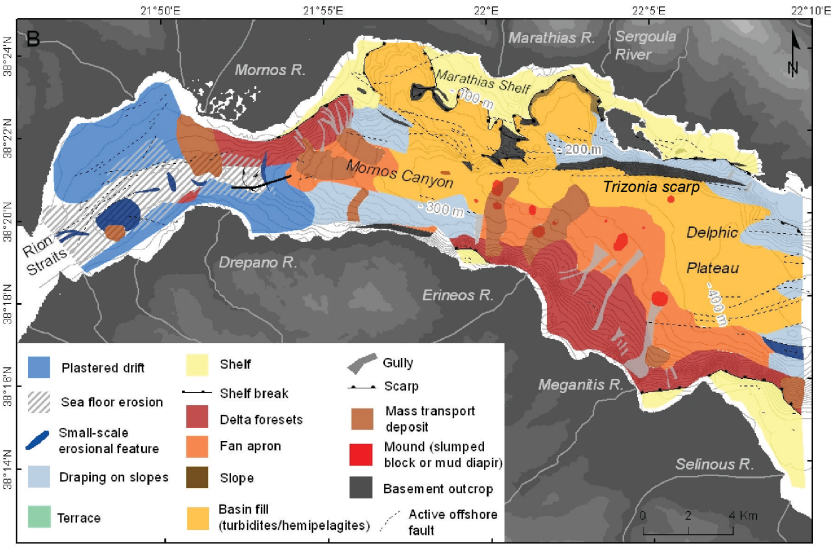

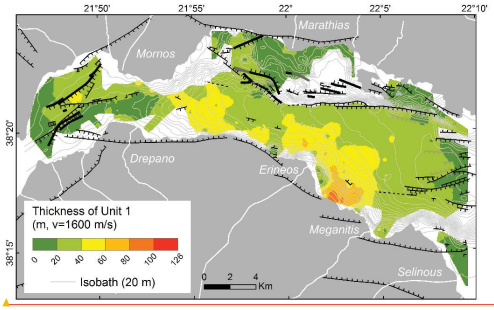

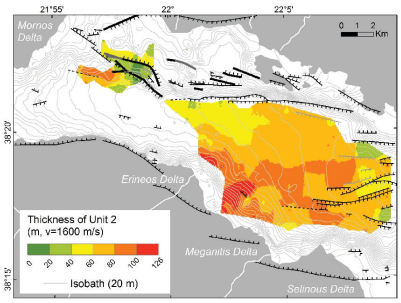

135

Unknown

Formatted: Font:Times New Roman, Bold

Figure 2. Inventory of mass transport deposits (MTDs) at the westernmost Gulf of Corinth for the last ca. 130 ka. A) spatial extent and age of the 32 MTDs with in grey seismic grid used for the inventory; B) to G): spatial distribution of MTDs for each sliding event (SE). Grey lines show the seismic grid. Black dots represents the mounds described in Beckers et al. (2016a). The total volume of sediments in the MTDs is

Aurélia Ferrari 13/2/2018 10:03
Deleted: 1

Aurélia Ferrari 13/2/2018 10:56
Deleted: .

145 mentioned for each sliding event.

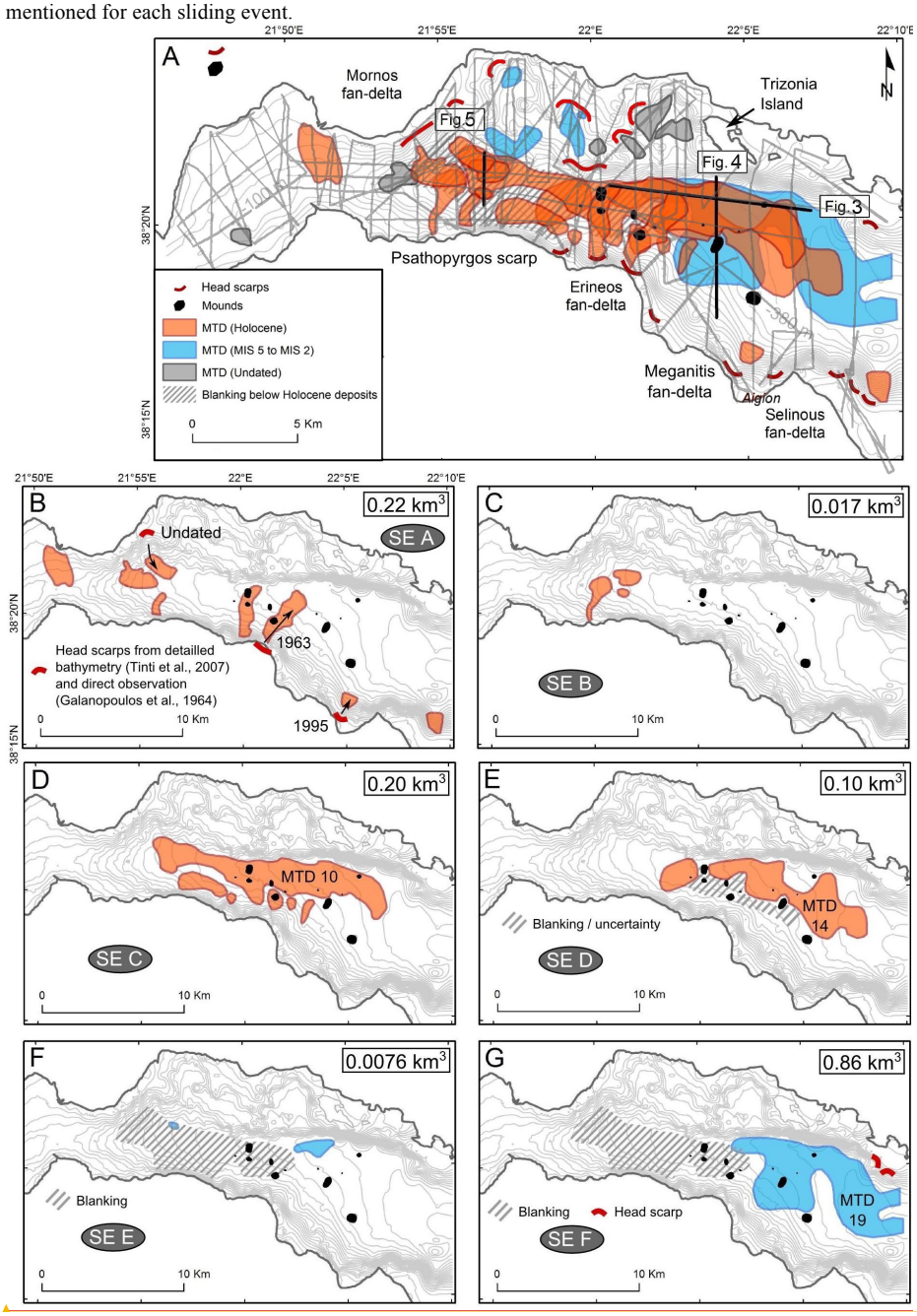

146
147
148

Unknown
Formatted: Font:Times New Roman

Aurélia Ferrari 13/2/2018 11:16

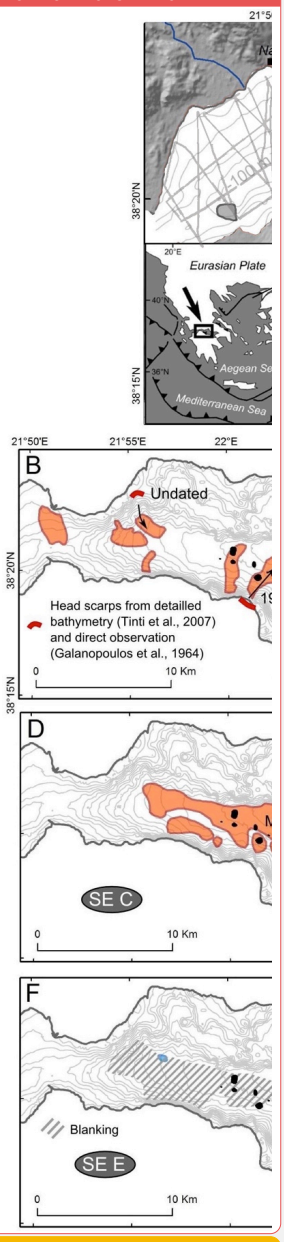

Deleted:

Unknown
Formatted: Font:Times New Roman

Mass transport deposits have been identified on high-resolution seismic profiles based on their typical seismic facies made of discontinuous to chaotic reflections. The shape of each deposit in map view has been interpolated manually, based on the seismic profiles that intersect the MTD. Thicknesses were derived using a seismic velocity of 1600 m s^{-1} (Bell et al., 2009). For the largest MTDs, an inverse distance weighted interpolation between thickness data points was used to derive isopach maps of the deposits and estimate their total volume. However, this interpolation method cannot be used for smaller MTDs crossed only by a few seismic lines. In this case, the volume was estimated by multiplying the MTD surface by an average thickness value. The derived volumes of small MTDs (surface area < ~2 km^2) are thus rough estimates, especially for MTDs crossed by only two or three seismic profiles. By contrast, volume estimates of large MTDs (surface area > ~5 km^2) are more accurate with volume uncertainties probably < 20 %.

Landslide headscarps have been mapped using three different data sources, namely (1) the grid of high-resolution seismic profiles acquired for this study, (2) an analysis of three submarine landslides in the study area by (Tinti et al., 2007), and (3) a 3D bathymetric view of the area between the Erineos and the Selinous fan-deltas from Lykousis et al. (2009). In the absence of multi-beam bathymetry over the whole study area, the mapping of Late Quaternary submarine landslides head scarps presented here is certainly not exhaustive. The location of potential headscarps associated with the largest MTDs mapped in the following are also discussed considering the location of the thickest deposits and the nearest upslope delta-front sediments.

4 Results

Thirty-two MTDs have been imaged in the study area, from which 67% are located in the large E-W trending basin located below the flat deep basin (Mornos Canyon and Delphic Plateau, Fig. 2). Eight MTDs have been identified in the northern margin of the Gulf, and two in the Nafpaktos Bay to the west of the Corinth Gulf (Fig. 2). The age of 24 MTDs has been estimated based on the stratigraphic framework developed previously (Beckers et al., 2015): 19 of them occurred during the Holocene and 5 during the period between ~130 ka and ~11.5 ka. A finer stratigraphy could be established in the flat deep basin, thanks to the relative continuity of the reflectors over this 20 km-wide area. Consequently, this work focuses on the 22 MTDs located in this area.

In the Delphic Plateau basin (eastern part of the deep flat basin), most MTDs are imaged as lenticular bodies of low-amplitude, incoherent reflections (Fig. 3 and 4). They generally have a flat upper surface and pinch out on their margins. Their thickness ranges between a few meters, which is the minimal thickness for a MTD to be imaged with the seismic system used, and 53 meters. The geometry and seismic facies indicate subaquatic mass-flow deposits (e.g. Moernaut et al., 2011, Strasser et al., 2013). The seismic facies of many MTDs also suggests a fine-grained lithology. However, this statement must be viewed cautiously considering the uncertainties on the interpretation of seismic facies in terms of grain-size, especially for reworked sediments. For instance, failure of coarse-grained deltaic deposits commonly result to their total disaggregation and transformation into grain flows and turbidity currents, whereas finer grained deposits evolve as landslides and cohesive debris flows (Tripsanas et al., 2008).

In the Mornos Canyon basin (western part of the deep flat basin), the MTDs present the same general characteristics but the reflector pattern is more variable (Fig. 5). Some high-amplitude reflections and coherent layering are observed in some MTDs, suggesting coarser-grained sediments and locally preserved stratigraphy.

Finally, some of the 22 MTDs show sediment/fluid escape features at their top (Fig. 3 and 5). Such features might have been produced by the combination of under-compaction (excess pore water pressure) and shaking, thus possibly pointing to paleoearthquakes (e.g. Moernaut et al., 2007, Moernaut et al., 2009). The volume of sediments in individual MTDs ranges from 7.7 10^5 to 8.6 10^8 m^3 (Fig. 6).

Landslide headscarps have been identified in different parts of the study area (Fig. 2A). They are particularly numerous on the slopes of the large Gilbert fan-deltas of the Erineos, Meganitis and

Aurélia Ferrari 21/2/2018 14:15
Deleted: Some potential l

Aurélia Ferrari 13/2/2018 10:52
Deleted: 1

Aurélia Ferrari 13/2/2018 10:52
Deleted: 1

Aurélia Ferrari 13/2/2018 10:52
Deleted: 2

Aurélia Ferrari 13/2/2018 10:53
Deleted: 3

Aurélia Ferrari 7/2/2018 15:17
Deleted: , which would make them different from the coarse-grained deltaic deposits that are known to fail relatively frequently along the southern coast

Aurélia Ferrari 13/2/2018 10:53
Deleted: 4

Aurélia Ferrari 7/2/2018 15:18
Deleted: revealing

Aurélia Ferrari 7/2/2018 15:18
Deleted: layering

Aurélia Ferrari 13/2/2018 10:53
Deleted: 2

Aurélia Ferrari 13/2/2018 10:53
Deleted: 4

Aurélia Ferrari 13/2/2018 10:56
Deleted: 5

Aurélia Ferrari 13/2/2018 10:53
Deleted: 1

Selinous at the south-east and Mornos at the north-west. In the latter area, one up to 50 m-high headscarp is imaged in the seismic data. The absence of undisturbed sediments on the erosional slope, downslope of the headscarp, suggests a recent age. In the Erineos, Meganitis and Selinous fan-delta slopes, headscarps have been identified in the seismic data and on the 3D view from Lykousis et al. (2009). Most of these headscarps are relatively small, lunate-shaped features linked to gullies (see also the bathymetric map in Fig.1). Two large head scarps are localized on the northern slope as well (Fig. 2A). Linking a headscarp to a particular MTD is often delicate for two reasons. First, the age of the headscarps is difficult to estimate because these erosional forms often affect steep slopes in coarse-grained deposits, making impossible to define a seismic stratigraphy in such areas. Second, at the foot of these erosional slopes, a high number of MTDs are stacked (e.g., Fig. 3). Exceptions, detailed hereafter, concern three recent submarine landslides and the largest observed MTD (MTD 19 in sliding event F).

Aurélia Ferrari 13/2/2018 10:53
Deleted: 1

Aurélia Ferrari 13/2/2018 10:53
Deleted: 2

Figure 3. E-W Sparker seismic profile showing the mass transport deposits imaged in the Delphic Plateau basin. See the location of the profile in Fig. 2. Horizon [1] indicates the beginning of the last post-glacial transgression, at 10.5-12.5 ka and horizon [2] the marine isotopic stage 6 to 5 transgression, which occurred at ca. 130 ka (Cotterill, 2006; Beckers et al., 2015; 2016)

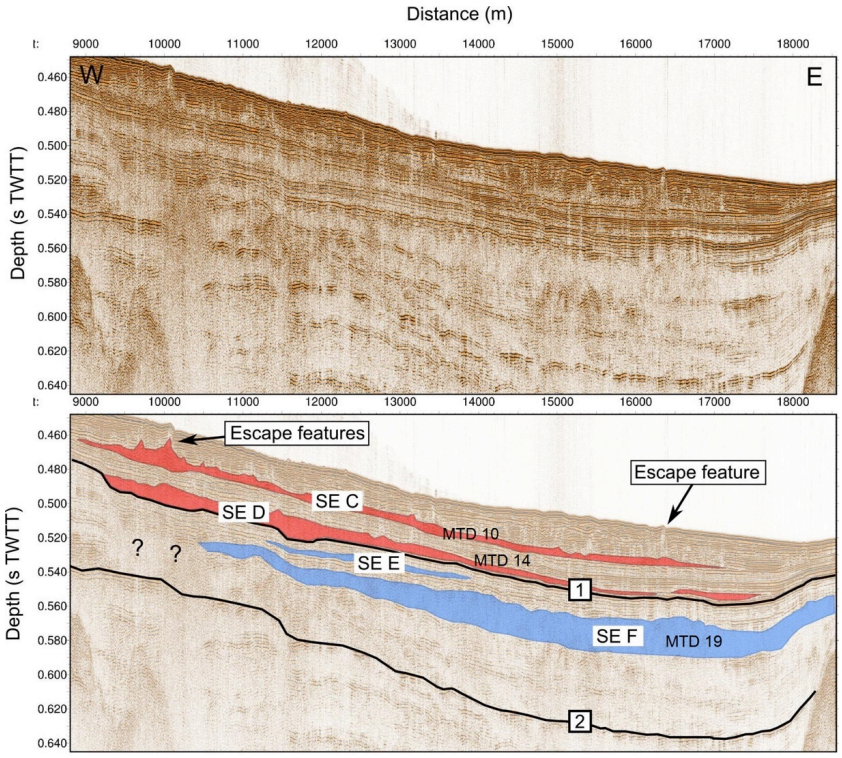

Aurélia Ferrari 13/2/2018 10:30
Deleted: 2

Aurélia Ferrari 13/2/2018 10:53
Deleted: 1

Figure 4. S-N Sparker seismic profile showing the mass transport deposits imaged in the Delphic Plateau basin. Questions marks highlight units of remobilized sediments that are difficult to localize in the stratigraphic framework. See the location of the profile in Fig. 2.

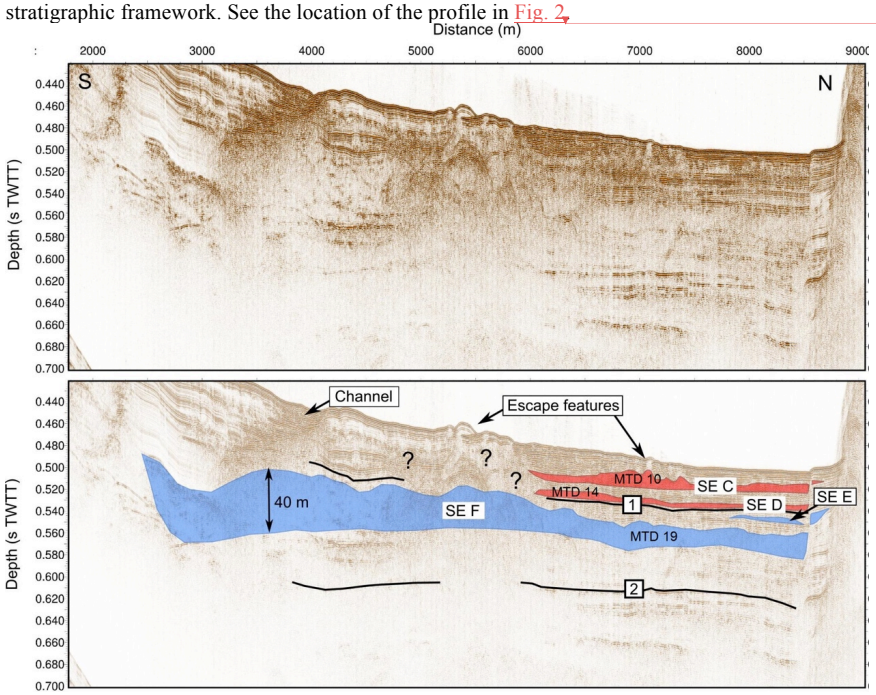

Aurélia Ferrari 13/2/2018 10:30
Deleted: 3

Aurélia Ferrari 13/2/2018 10:53
Deleted: 1

Figure 5. Examples of mass transport deposits in the Canyon basin. See the location of the Sparker seismic profile in Fig. 2

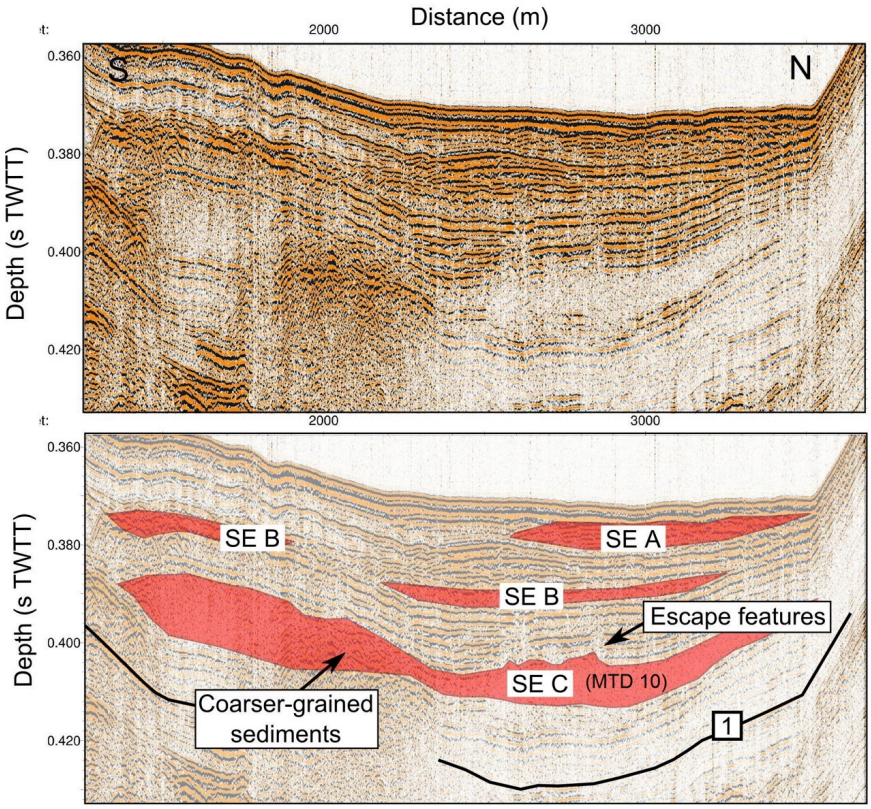

Figure 6. Volume distribution of the 22 MTDs studied in the Canyon and the Delphic Plateau basins. The names given to the three largest MTDs correspond to the notation in Fig. 2.

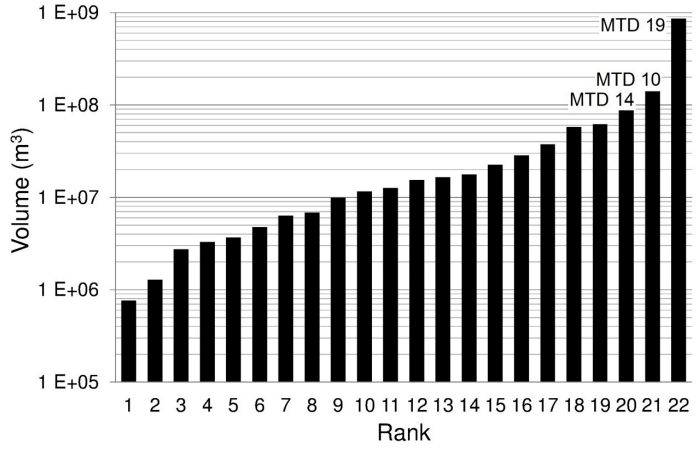

Aurélia Ferrari 13/2/2018 10:30
Deleted: 4

Aurélia Ferrari 13/2/2018 10:54
Deleted: 1

Aurélia Ferrari 13/2/2018 10:30
Deleted: 5

Aurélia Ferrari 13/2/2018 10:54
Deleted: 1

The stratigraphic position of MTDs in the Canyon and in the Delphic Plateau basins is not random. Most of them are clustered and are defining multi-MTDs temporal "events", based on common un-deformed underlying or overlying reflections that can be followed across the basin. Such correlations suggest that six events of large clustered submarine mass wasting occurred over the last 130 ka. Two sliding events (SE) are represented by clustered MTDs located between reflectors 2 and 1 (SE E and F). The four others occurred during the Holocene: SE D comprises MTDs deposited just on top of the reflector 1, SE C is located in the middle of the Holocene sequence, SE B somewhat higher, and finally SE A includes MTDs at or near the sea floor responsible for its present-day hummocky topography. The spatial distribution and the total volume of the MTDs associated to each of these events are represented in Fig. 2.

In some zones (Fig. 2), the existence or the geometry of MTDs is difficult to evaluate because of seismic blanking and strong chaotic reflections affecting some stratigraphic intervals. Above reflector 1, the stratigraphy is clear except regarding the southern extension of MTD 14 in SE D. The low amplitude, almost transparent reflections characterizing the MTD deposit extends until a more chaotic and thicker deposit associated with surface mounds (Fig. 4). We could not decipher if the chaotic reflections that disturb the seismic stratigraphy was associated with MTD 14 in SE D or in relation with sediment remobilization from the underlying sliding event F (Figs. 4 and 5). So the mapped extension of MTD 14 in Fig. 2E is conservative and considered as a minimum. Below reflector 1, the amplitude of the reflectivity sharply decreases, which is a characteristic of lowstand deposits in the Gulf (Bell et al., 2008), and blanking occurs in two areas. In the Mornos Canyon area, a wide blanking area exists at a depth of about 50 to 70 m below the sea floor, a few meters below reflector 1, in direct continuity with the delta of the Mornos River. Blanking is thus a low-stand related feature and might correspond to coarse grained, organic rich sediments of the Mornos River. Consequently, the stratigraphy of MTDs between reflectors 2 and 1 is well established only below the Delphic Plateau. The other area associating with blanking and strongly disturbed sediments forming mounds occurs at the junction between the Mornos Canyon and the Delphic plateau at the foot of the Erineos foreset beds, at a depth similar to SE F. Its origin is unknown, but it might be related to an MTD deposit in relation with MTD 19.

The definition of sliding events reflects a clustering of submarine landslides in a relatively short period of time. It does not necessarily imply a synchronous occurrence of all submarine landslides included in one event. Indeed, the accuracy of the correlation between separated MTDs that are interpreted to belong to the same sliding event is in the order of one or two reflections in the seismic data. Deciphering the exact MTD chronology within a sliding event was not possible because of the discontinuous character of many reflections and the relatively large distance that separates some MTDs (up to 8.5 km). This "stratigraphical" uncertainty corresponds to ~1-2 meters of sediment or, based on sedimentation rate estimates, sliding events represent a set of MTDs that occurs over a period of 300 to 1000 years (Lykousis et al., 2007).

Individual sliding events are characterized as follows (Fig. 2B to G):

Sliding event A: Eight MTDs at or near the sea floor have been identified. Their spatial distribution indicates that three of them result from slope failures in the Mornos delta and five from failures at different locations along the southern margin (Fig. 2). The volumes of these MTDs range between ~4.7 10^6 m^3 and ~6.2 10^7 m^3, and the total volume of the eight MTDs is about ~2.2 10^8 m^3.

Some of these MTDs correspond to submarine landslides described in the literature (Galanopoulos 1964; Papatheodorou and Ferentinos 1997; Tinti et al., 2007). The MTD located north-east of the Erineos delta results from a coastal landslide on this fan-delta in 1963, which triggered a large tsunami on both sides of the Gulf (Galanopoulos et al., 1964; Stefatos et al., 2006). The MTD located at the foot of the Meganitis fan-delta likely corresponds to a coastal landslide triggered by the 1995 Aigion earthquake on this delta (Papatheodorou and Ferentinos 1997; Tinti et al., 2007). The volumes of sediments involved in these two landslides have been estimated at ~4.6 10^7 m^3 from the data presented by Stefatos et al. (2006), and about ~2.8 10^7 m^3 by Tinti et al. (2007), respectively. The corresponding volumes estimated from the present study are ~6.1 10^7 m^3 and ~2.2 10^7 m^3, which are in the same order

Aurélia Ferrari 7/2/2018 15:24
Deleted: may be assigned to

Aurélia Ferrari 7/2/2018 15:30
Deleted: that outcrop

Aurélia Ferrari 13/2/2018 10:54
Deleted: 1

Aurélia Ferrari 13/2/2018 10:55
Deleted: 1

Aurélia Ferrari 6/2/2018 10:59
Deleted:

Aurélia Ferrari 6/2/2018 11:01
Deleted: This so far poorly understood blanking area might correspond to a large MTD from the sliding events E or F, or to coarse-grained fluvio-deltaic deposits.

Aurélia Ferrari 21/2/2018 14:25
Deleted: However, there, the spatial extent of the MTDs from SE D (Fig. 1E) is uncertain, owing to chaotic reflections that disturb the seismic stratigraphy possibly in relation with sediment remobilization from the underlying sliding event F (Fig. 3).

Aurélia Ferrari 7/2/2018 15:28
Deleted: This uncertainty results from

Aurélia Ferrari 7/2/2018 15:29
Deleted: of sedimentation

Aurélia Ferrari 13/2/2018 10:54
Deleted: 1

Aurélia Ferrari 7/2/2018 15:31
Deleted: that outcrop

Aurélia Ferrari 13/2/2018 10:54
Deleted: 1

of magnitude. Another well preserved but undated landslide headscarp has been identified by Tinti et al. (2007) on the eastern side of the Mornos fan-delta (Fig. 2). These authors estimated the volume of the sliding mass at ~9 10^6 m^3. Our data show a MTD located about 1 km downslope of the scarp, with an estimated volume of ~9.9 10^6 m^3 that fits remarkably well with the volume derived from the geometry of the scarp.

Sliding event B: The sliding event B comprises three MTDs located at the western tip of the canyon. They are located between 12 and 16 m below the sea floor and are relatively thin (~2 to 5 m thick) (Fig. 5). Location and geometry of the MTDs indicate that they result from slope failures in the Mornos fan-delta and in the Psathopyrgos scarp. The total volume of these MTDs is about ~1.7 10^7 m^3.

Sliding event C: The sliding event C includes one large MTD extending over a wide area below the Mornos Canyon and a part of the Delphic Plateau (MTD 10), and smaller deposits located at the foot of the southern slopes, in the Psathopyrgos scarp and Erineos fan-delta areas. The thickness of MTD 10 is shown in Fig. 7. Five local maxima are connected by a 2-5 m thick sheet of low-amplitude incoherent reflections. The thickest sediment accumulation (30 m) is located at the foot of the Erineos fan-delta. The other maxima are 5 to 10 m thick. Two are located at the western tip of the MTD and suggest sediment inputs from the Mornos fan-delta area and from the Psathopyrgos scarp (Fig. 5). The last two maxima are located in the south-eastern part of the deposit, with a possible source in the Erineos fan-delta (Fig. 7). The total volume that failed during sliding event C is about ~2.0 10^8 m^3, including ~1.4 10^8 m^3 for MTD 10.

Figure 7. Thickness of the largest MTDs deduced from the interpretation of Sparker seismic profiles with probable sediment paths indicated by red arrows (bold arrow: main sources). Contours represent the sea floor bathymetry interpolated from the Sparker data (one line every 20 m). Left: MDT 10 in sliding event C, the largest MDT from the sliding event C. Center: Thickness of MDT 14, the largest of the two MTDs that define the sliding event D. Bottom: The largest MTD from the presented inventory (MTD 10, sliding event F). The black bold lines represent two landslide head scarps likely linked to the MTD. The dotted line shows the location of the seismic profile in Fig. 8.

Aurélia Ferrari 13/2/2018 10:58
Deleted: 1

Aurélia Ferrari 13/2/2018 10:58
Deleted: 4

Aurélia Ferrari 13/2/2018 10:58
Deleted: 6

Aurélia Ferrari 13/2/2018 10:58
Deleted: 4

Aurélia Ferrari 13/2/2018 10:30
Deleted: **6**

Aurélia Ferrari 21/2/2018 14:28
Formatted: Font:Not Bold

Aurélia Ferrari 21/2/2018 14:28
Deleted: Thickness of

Aurélia Ferrari 21/2/2018 14:29
Deleted: , deduced from the interpretation of Sparker seismic profiles

Aurélia Ferrari 21/2/2018 14:30
Deleted: Contours represent the sea floor bathymetry (one line every 20 m). MoF = Mornos fan-delta, ErF = Erineos fan-delta, MeF = Meganitis fan-delta.

Aurélia Ferrari 21/2/2018 14:30
Deleted: , deduced from the interpretation of Sparker seismic profiles. Contours represent the sea floor bathymetry (one line every 20 m). ErF = Erineos fan-delta.

Aurélia Ferrari 21/2/2018 14:31
Deleted: ... [1]

Aurélia Ferrari 13/2/2018 10:58
Deleted: 7. EF = Erineos fan-delta, SF = Selinous fan-delta.

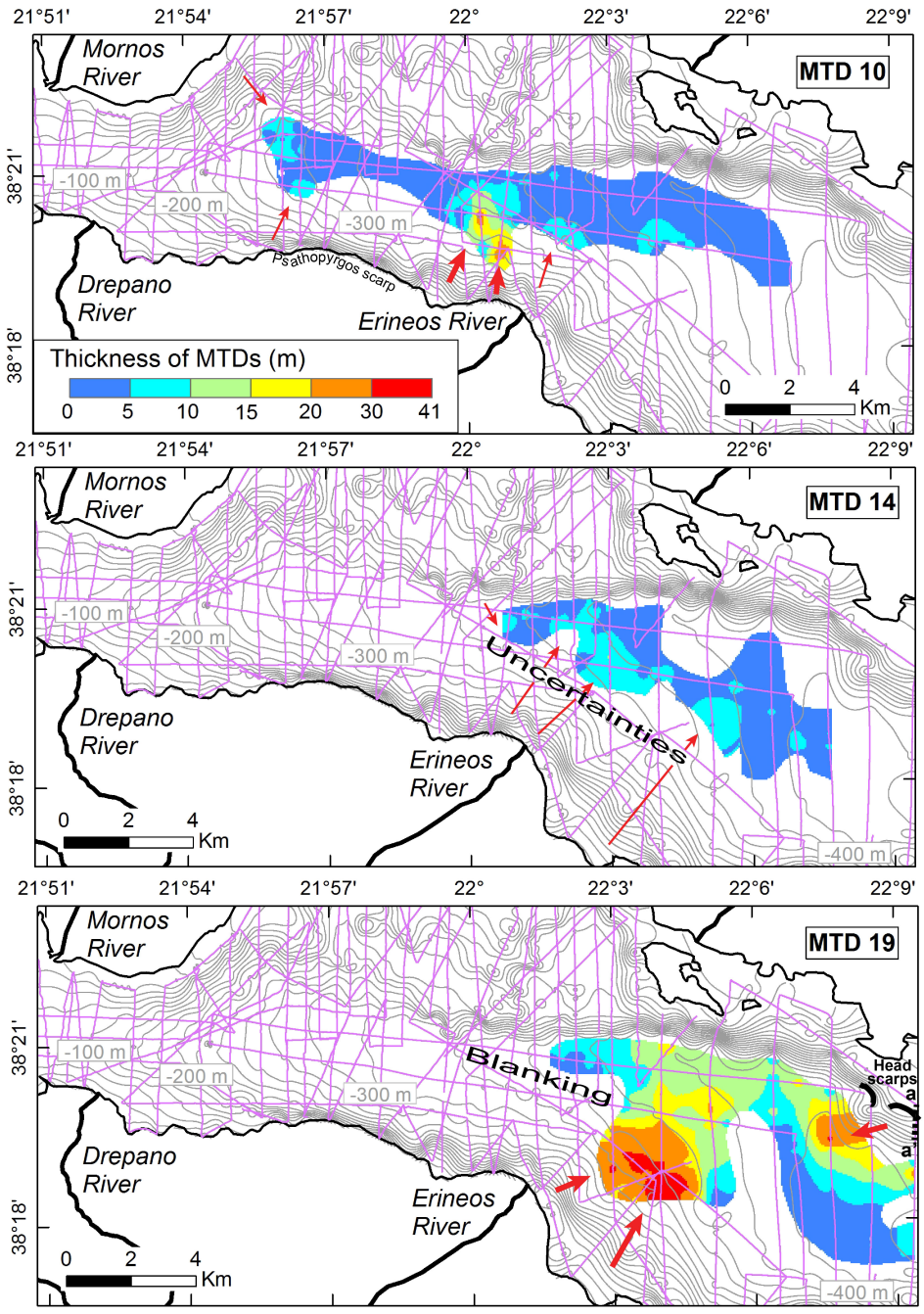

Unknown

Formatted: Font:Times New Roman

Aurélia Ferrari 9/2/2018 12:00

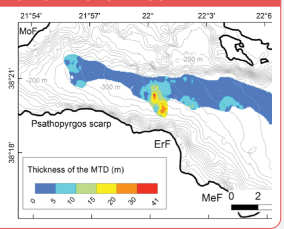

Deleted:

The geometry of MTD 10 suggests that slope failures occurred simultaneously in different parts of the westernmost gulf during sliding event C. The main source of sediment was the Erineos fan-delta, as attested by the location of the thickest sediment accumulation in the MTD 10, and by the presence of other MTDs at the same stratigraphic level between MTD 10 and the Erineos fan-delta (Fig. 2D).

Sliding event D: Two MTDs are located just on top of reflector 1 and define the sliding event D. Both are between ~2 and 10 m thick and spread over several square kilometres in front of the Erineos and Meganitis fan-deltas. The southern limit of the deposits is unclear, because the stratigraphy in the area between the two MTDs and the Erineos pro-delta is poorly constrained (hatching on Fig. 2E and question marks in Fig. 4). In this area, it is not sure whether the incoherent reflections located south of the SE D MTD at a similar depth represent the same MTD or the underlying, older (SE F), MTD or escape features from the latter, as suggested by the escape features observed at the sea floor (Fig. 4).

The isopach map of the largest deposit (MTD 14) is shown in Fig. 7 and suggests that it was fed by slope failure(s) mostly south of the Delphic Plateau probably from the Erineos Delta Fan. The volume of MTD 14 is estimated at ~8.7 10^7 m^3, and the total volume of SE D MTDs is about ~1.0 10^8 m^3. Considering uncertainties on the geometry of these MTDs' southern edges, these values are minimum estimates.

Sliding event E: Two MTDs define this sliding event. The largest one is located in the Delphic Plateau basin, just south of the Trizonia Island and has a volume of ~6.6 10^6 m^3. The second is much smaller (~1.3 10^6 m^3) and is located in the Canyon basin. Stratigraphically, both are located a few meters below reflector 1. However, they are horizontally 8.5 km apart, making the correlation uncertain. The total volume of the two MTDs in sliding event E is ~7.9 10^6 m^3.

Sliding event F: The sliding event F is defined by one single large complex MTD (MTD19) (Fig. 2). This deposit is located in the Delphic Plateau basin. Stratigraphically, it belongs to the upper part of the unit between reflectors 2 and 1, suggesting that this event occurred during the last glacial period. With a volume of ~8.6 10^8 m^3, this deposit is the largest MTD of the present inventory. It covers an area of 41 km^2, i.e., almost the whole Delphic Plateau. The isopach map reveals a main up to 50 m-thick sediment accumulation in the south-western part of the deposit (Fig. 4) and another ~30 m-thick depocenter in the north-eastern part (Fig. 7). The MTD is imaged as low amplitude, almost transparent chaotic reflections except in the thickest part where high-amplitude reflections could indicate coarser-grained sediments and locally preserved layering (Fig. 4). No sedimentological structure has been observed in the seismic profiles between the two maxima in thickness.

The geometry of the deposit and the absence of clear structure between the two depocenters support the idea of at least two simultaneous slope failures having generated this large MTD. The largest failure occurred south of the MTD, on the Meganitis or the Erineos fan-delta slopes. Considering the large volume of sediments in the south-western part of the MTD, we expected a major scar across the southern slopes, which we could not retrieve however neither from the seismic data, nor from published bathymetries (Lykousis et al., 2009; Nomikou et al., 2011, see our Fig. 1). Indeed, dozens of small head scarps and gullies dissect the slopes of the offshore Erineos and Meganitis deltas, making difficult the identification of large features. The second depocenter occurs near the north-eastern edge of the Delphic Plateau Basin, and upslope two submarine landslide headscarps located 2 km from each other were evidenced in seismic profiles (bold lines in Fig. 7). Cut through stratified hemipelagites, they are 11 and 15 m-high and are located at 300 and 195 m below the sea level, respectively (Fig. 8). Although it is not possible to reconstruct the 3D geometry of a single large headscarp from the seismic data, this would be a good candidate source of the thick sediment accumulation in the north-eastern part of MTD 19.

Figure 8. Sparker seismic profile illustrating a submarine landslide head scarp that is probably linked to the MTD 19. See the location of the profile in Fig. 7.

Aurélia Ferrari 13/2/2018 10:58
Deleted: 1

Aurélia Ferrari 13/2/2018 10:58
Deleted: 1

Aurélia Ferrari 13/2/2018 10:58
Deleted: 3

Aurélia Ferrari 13/2/2018 10:59
Deleted: 3

Aurélia Ferrari 13/2/2018 10:59
Deleted: 6

Aurélia Ferrari 13/2/2018 10:59
Deleted: 1

Aurélia Ferrari 13/2/2018 10:59
Deleted: 3

Aurélia Ferrari 13/2/2018 10:59
Deleted: 6

Aurélia Ferrari 13/2/2018 10:59
Deleted: 3

Aurélia Ferrari 21/2/2018 14:46
Deleted: T

Aurélia Ferrari 21/2/2018 14:46
Deleted: are highlighted

Aurélia Ferrari 21/2/2018 14:46
Deleted: by

Aurélia Ferrari 21/2/2018 14:46
Deleted: on the slope north of the MTD

Aurélia Ferrari 13/2/2018 10:59
Deleted: 6

Aurélia Ferrari 13/2/2018 11:00
Deleted: 7

Aurélia Ferrari 21/2/2018 14:47
Deleted: might

Aurélia Ferrari 13/2/2018 10:31
Deleted: 7

Aurélia Ferrari 13/2/2018 11:00
Deleted: 6

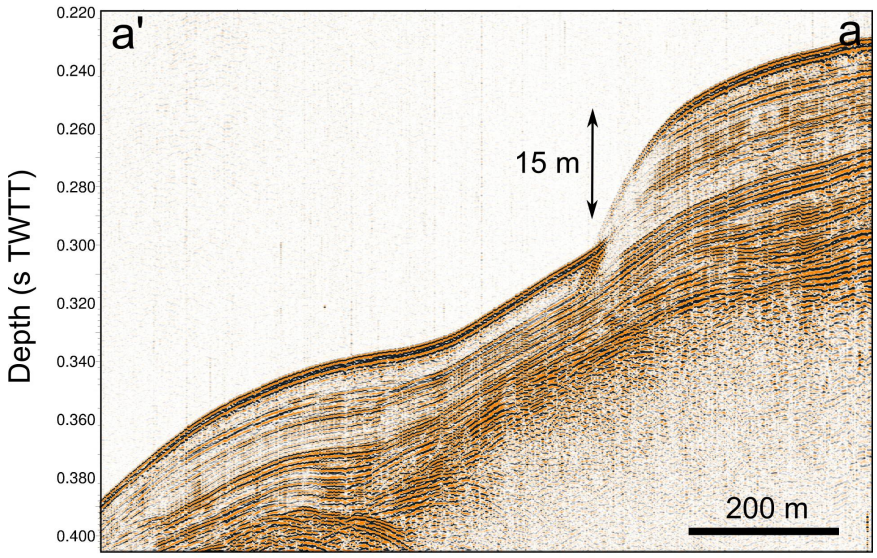

5 Discussion

5.1 Limitations of the analysis

Before discussing the implications of the presented MTD inventory in the deep flat basin in terms of sediment sources and triggering mechanisms, it is necessary to point out that only submarine landslides that have remobilized a sufficient quantity of sediments down to the basin floor are considered here. Moreover, the high-resolution seismic profiling system used does not permit identifying MTDs thinner than ~1 m. Consequently, our inventory is incomplete and could be refined by the use of very-high resolution seismic profiling systems and long cores.

5.2 Sediment sources

According to the mapping of the thickness of the deposits, large sliding events in the westernmost Gulf of Corinth mainly result from slope failures in, or close to, the Gilbert-type fan-deltas. Large sediment volumes were trapped in these deltas during the Holocene. As shown in Figure 1, Holocene foreset beds reach 40 to 60 m in thickness on average in the Eroneos and Meganitis fan-deltas, and sediment accumulation during the Holocene exceeding 100 m have been observed locally in between. These are the sources of MTD 10 in sliding event C and MTD 14 in sliding event D. The remarkable amount of sediments delivered to the gulf of Corinth during the Holocene probably results from large volumes of sediments stored onland during the last glacial period that were mobilized from river floodplains and colluvial deposits to rivers deltas. Widespread soil erosion resulting from human deforestation and agriculture during the second half of the Holocene also contributed to increase sediment fluxes in this period. Similarly, the previous period considered here spanning ~130 ka to ~11 ka is also characterized by a large sediment accummulation with a pile of 60 to 120 m forming the delta fronts of the Erineos and Meganitis delta (Fig. 1). These sources are some of the main source of MTD 10 in sliding event F.

The seismic facies of most large MTDs also implies that they are likely composed mainly of fine-grained sediments, and seismic profiles across fan-delta area have shown that the pro-delta foresets are locally made of a thick accumulation of stratified fine-grained sediments. These fan-delta sediments are probably the main source of sediments for the largest MTDs (MTD 10, 14 and 19). However, some smaller MTDs seem to be made of coarser-grained sediments according to the seismic character (e.g., in

Aurélia Ferrari 7/2/2018 15:09
Deleted: However,

Aurélia Ferrari 7/2/2018 15:09
Deleted: t

Aurélia Ferrari 7/2/2018 15:09
Deleted: rather than gravels typical of fan-deltas. S

Aurélia Ferrari 7/2/2018 15:10
Deleted: in the Erineos

Aurélia Ferrari 7/2/2018 15:11
Deleted: up to 90 m thick for the Holocene unit. Preserved between large gullies, these sediments display a surface slope of ~6°

Aurélia Ferrari 7/2/2018 15:11
Deleted: They

SEs A and B in the Mornos Canyon basin), suggesting failure also occurred in coarser-grained parts of the fan-deltas located at the junction between the topset and the foreset beds (e.g., the 1963 slide in the Erineos fan-delta).

5.3 Significance of the sliding events

The data suggest that large submarine landslides have been triggered during six short periods of time over the last 130 ka. These sliding events include variable numbers of clustered MTDs, from one (SE F) to 8 (SE A). During three sliding events (C, D, F), a particularly large MTD accumulated at the basin floor, and it has been shown that these large MTDs resulted from several possibly synchronous slope failures. Similar MTD distributions have been observed in lakes in the Alps and in the Chilean Andes (Strasser et al., 2013; Moernaut et al., 2007). In these studies, the correlation of MTDs into a same "sliding event" was supported by radiocarbon dating and a simultaneous triggering has been proposed. Correlations between the mass wasting records of neighbour lakes and the historical seismicity revealed that most of these "sliding events" had been triggered by large earthquakes (Strasser et al., 2006; Moernaut et al., 2007). In the westernmost Gulf of Corinth, neither coring, nor dating is available to confirm our correlations between MTDs. Moreover, the occurrence of frequent turbidity currents (Heezen et al., 1966; Lykousis et al., 2007a) and small-scale submarine landslides perturbs the sediment layering and induces discontinuities in the seismic reflections, which makes MTD correlations based on the seismic stratigraphy less accurate there than in many lakes.

The case of sliding event A demonstrates that MTDs grouped within the same event did not necessarily occur at the same moment. Indeed, direct observation has shown that one MTD of this event occurred in 1963 AD and another in 1995 AD. By contrast, the synchronicity of different submarine landslides has been suggested for SE C, D and F from the complex shape of the large MTDs they include. Though not a proof, this lends support to the hypothesis of a seismic trigger of these three sliding events.

Consequently, the sliding events defined in this study may represent two different situations. In a first case, they correspond to a period of time of 0.3 to 1 ka during which several submarine landslides of various origins occurred. The sliding event A is such a case, with the coastal landslide caused in the Meganitis delta area by the 1995 Aigion earthquake and an aseismic coastal landslide in the Erineos delta area in 1963. The second case refers to likely simultaneous submarine landslides originating from different slopes and forming a wide MTD of complex shape in the basin floor. An example of this case, which is proposed to be earthquake-triggered, is the sliding event F, with a single MTD of complex shape. Sliding events C and D possibly belong to this category as well. There is insufficient data to allow for the determination of the nature of the minor events B and E.

Two main questions arise from these observations.
- Is seismicity the only forcing of SEs C, D and F or could other triggers or pre-conditioning factors such as sediment supply and sea level change have influenced the system?
- What are possible trigger mechanisms and/or pre-conditioning factors responsible for a cluster of slope failures such as SE A?

Urlaub et al. (2013) make inferences about controls on triggers of submarine landsliding from the statistical analysis of the ages of 68 very large slides (> 1 km^3) around the world. From a subset of 41 slides that occurred during the best documented last 30 ky, they show that the distribution of number of events per ky resembles a Poisson distribution, suggesting that large submarine mass wasting might be essentially random or, at best, that the global-scale signal for a climatic control, through either sea level or sedimentation rate changes, is incoherent (non-uniform response of continental slopes worldwide) or too weak to be expressed clearly with such a small sample size. They also note that, though strong earthquakes might represent a temporally random trigger at the global scale, most of the slides in their data set are located in low-seismicity passive continental margins (Urlaub et al., 2013). Here, we first investigate the possible role of earthquakes through a comparative analysis of the frequency of sliding events and earthquakes in the Gulf of Corinth area. Then, other potential controls will be discussed by comparing the age distribution of the largest sliding events with published data about changes in

sediment dynamics and marine conditions in the Corinth Rift area. Owing to the small number of events and high age uncertainties, which rule out statistical considerations, we provide only a qualitative analysis.

5.4. The possible role of large earthquakes

The last four sliding events occurred during the last 10-12 ka, at an average rate of one event every 2.5-3 ka. Only two sliding events have been detected between ca. 130 ka and 10-12 ka. This high Holocene frequency compared with the ~120 kyrs anterior period may be attributed to two factors. First it might be a bias because the seismic reflections corresponding to the last glacial period (110-12ka) are less clear (lower amplitude and lower continuity) than the reflections from the Holocene interval. Consequently, medium-sized landslides such as those detected in SEs A and B might have been missed in the seismic unit between reflectors 2 and 1. Second, it could be attributed to a change in earthquake frequency due to a Holocene acceleration of the strain rates that was evidenced by fluvial morphometry (Demoulin et al., 2015) and subsidence markers (Beckers, 2015).

The average recurrence interval for large earthquakes (Mw 6-7) has been estimated in the central part of the Gulf of Corinth at ~500 yr during the Holocene, and ~400 yr for the period 12-17 ka, based on the record of "homogenites" in the deepest part of the Gulf (Campos et al., 2013). In the western Gulf of Corinth, estimates from palaeoseismological trenches on individual faults suggest an average recurrence interval ≤ 360 yr on the Aigion fault (Pantosti et al., 2004), and of 200-600 yr on the East Helike fault (McNeill et al., 2005) for the past 0.5-1 ka. It is clear, therefore, that large sliding events in the westernmost Gulf of Corinth were less frequent than Mw 6-7 earthquakes, during both the Holocene and the last glacial period. Consequently, while (anomalously?) large earthquakes could have triggered SEs C, D and F, as suggested above from the geometry of MTDs 10, 14 and 19, it is likely that other factors contributed to the occurrence of such large sliding events. These factors are explored in the next section.

5.5 Other potential triggers and pre-conditioning factors

Other possible processes that might have "pre-conditioned" or triggered sliding events in the Gulf of Corinth need to show a return period of at least 2.5 ka over the last 12 ka in order to fit the SE frequency. The following processes are proposed:
1. Sediment loading on top of a weak layer (e.g., gas-filled muddy sediments, as suggested for the area by Lykousis et al. (2009)) (pre-conditioning factor);
2. Pulses of increased onshore erosion inducing temporary increase of sedimentation offshore, in turn leading to slope overloading (pre-conditioning factor);
3. Sea level changes, which would have favoured slope failures during either lowstand conditions (Perissoratis et al., 2000) or sea level rises (Zitter et al., 2012) (pre-conditionning factor);
4. Changes in the circulation and/or intensity of bottom-currents progressively destabilizing submarine slopes through an increase in sedimentation or erosion rate (pre-conditioning factor);
5. Middle-term tectonic pulses, which would have temporarily increased the level of regional seismicity (Koukouvelas et al., 2005; Demoulin et al., 2015) (trigger);
6. Loading by exceptional storm waves (trigger);
7. Large supply of coarse-grained sediments at a river mouth during exceptional flooding events inducing slope failures by sediment overloading, as attested for the 1963 coastal landslide on the Erineos fan-delta by Galanopoulos et al. (1964) (trigger).

All these hypotheses are not directly testable. Moreover, it is likely that different pre-conditioning factors and triggers have interacted in various ways over the last 130 ka. Nevertheless, the four proposed pre-conditioning factors can be discussed by comparing the SE age distribution with independent data available for the region. We focus on the four events that mobilized a large volume of sediment ($\geq 10^8$ m^3, SEs A, C, D, and F) because they probably indicate slope failures in different parts of the westernmost Gulf, thus pointing to a regional signal. Even though these events have not been directly dated by coring, ages can be reasonably inferred from the seismic stratigraphy. The most recent sliding event (SE A) comprises MTDs at or near the sea floor and consequently occurred in the last 0.3-1 ka (a

Aurélia Ferrari 21/3/2018 16:56
Deleted: a priori surprising low

Aurélia Ferrari 21/3/2018 16:56
Formatted: Font:Not Italic

Aurélia Ferrari 21/3/2018 16:56
Formatted: Font:Not Italic

Aurélia Ferrari 21/3/2018 16:57
Deleted: during the last glacial period (110-12 ka) with respect to the Holocene might actually be somewhat

Aurélia Ferrari 21/3/2018 16:57
Deleted: ed

Aurélia Ferrari 21/3/2018 16:57
Deleted: y the fact that

Aurélia Ferrari 21/3/2018 16:57
Deleted: that

Aurélia Ferrari 7/2/2018 15:32
Deleted: that outcrop

range accounting for the thin layer of hemipelagites possibly covering some MTDs). Sliding event C likely dates from the Mid-Holocene (~6-7 ka) according to the Holocene age-depth curve in the central part of the Gulf of Corinth (Campos et al., 2013). The two MTDs defining SE D occurred just after the lacustrine to marine transition at the end of the Last Glacial, around 10-12 ka. Finally, the sliding event F dates from sometime in the last glacial period.

Among the listed pre-conditioning factors, onshore erosion dynamics in the Corinth Rift area is the best temporally documented. Fuchs (2007) presents the evolution of sedimentation rates in colluvial deposits on the southern shoulder of the Corinth Rift, in the Phlious Basin, 25 km south of Xylocastro, for the last 10 ka (Fig. 9). He identifies two main phases of land degradation between 6.5 and 8.5 ka, and from ~4 ka onwards. While the age of SE A corresponds to the end of the most recent period of land degradation, the much more uncertain age of SE C could correspond to the end of the land degradation phase at 6.5-8.5 ka (Fig. 9). The sliding event D is too old to be compared with the results of Fuchs (2007). In brief, a relation might exist between periods of high sediment supply from the watersheds and the occurrence of sliding events during the last 10 ky (hypotheses 1 and 2).

Less information is available about Late Pleistocene sediment dynamics in the area. Collier et al. (2000) suggest that the denudation rate at the eastern end of the Gulf in the Alkyonides Basin during the last glacial period (12-70 ka) was almost twice those of the Holocene and MIS 5 interglacials. Instead, six radiocarbon dates on long cores in the center of the Gulf of Corinth show a moderate increase in sedimentation rate between the end of the last glacial period (17- 12 ka) and the Holocene (Campos et al., 2013). Overall, these data suggest that the Last Glacial probably experienced the largest sedimentation rates over the last 130 ka in most of the Gulf of Corinth. This inference is however not valid at the western tip of the Gulf. The comparison between isopach maps of the Holocene and the anterior 130-12 kyrs period evidences a large Holocene increase in sedimentation accumulation rate (Fig. 1). In the Delphic plateau basin, average sedimentation rate (excluding the thickness of MTDs) reaches ~2.4 mm/yr for the Holocene and ~ 0.4 mm/yr for the previous 120 kyrs. This is in line with the fact that only one large sliding event F was recorded during the ~60 ky-long Last Glacial. Increased sedimentation is thus a pre-conditioning factor of landsliding in the western Gulf.

Beside changes in erosion rates in the watersheds, the offshore realm underwent large changes between the last glacial period and today. From 70 to 12 ka, the Gulf of Corinth was a lake and the water level was around -60 m, assuming a constant depth of the Rion Sill over this period (Perissoratis et al., 2000). During this lowstand period, the extent of submarine slopes where submarine landslides can initiate were not significantly reduced, because the foreset beds of the Erineos and Meganitis that are the largest source of mass wasting sediments for the Delphic plateau extend down to the ~300 m isobaths. The steepest slopes of these two prodeltas are located above isobaths -100m and between isobaths -150m and -200m according to the slope map of Nomikou et al. (2011), so unstable slopes above -60m that were submerged only in the postglacial period cover a restricted area. At 10-12 ka, the rising waters in the Ionian Sea flooded the "Lake Corinth" through the Rion Sill (Moretti et al., 2003; VanWelden 2007). The sea level continued to increase from ca. -60 m to its present elevation until 5.5-6 ka, and bottom currents appeared in the study area (Beckers et al., 2016). The deposition of SE D occurred at 10-12 ka, when the water level started to increase in the Corinth Gulf. Water level change might change the stress field and pore pressure potentially affecting the earthquake cycle. Water level increase and bottom current initiation would also have favoured the destabilization of sediments deposited during the preceding glacial period. In the Sea of Marmara, observations by Zitter et al. (2012) and Beck et al. (2007) show an increase in large mass wasting events at the end of the last lacustrine period and at the beginning of the marine period that likewise can be explained by a change in oceanographic conditions, confirming the possible control of these pre-conditioning factors on SE D.

Figure 9. Comparison between the erosion dynamics over the last 10 ka from colluvial and alluvial archives in the Peloponnese (Fuchs, 2007), the rate of local water level changes, and the occurrence of large sliding

Aurélia Ferrari 13/2/2018 11:00
Deleted: 8

Aurélia Ferrari 13/2/2018 11:00
Deleted: 8

Aurélia Ferrari 21/3/2018 16:59
Deleted: While the occurrence of the major SE F during this period again lends support to

Aurélia Ferrari 21/3/2018 16:59
Deleted: i

Aurélia Ferrari 21/3/2018 16:59
Deleted: as

Aurélia Ferrari 21/3/2018 16:59
Deleted: , it may however be surprising that no other large sliding event has been recorded under such circumstances during the ~60 ky-long Last Glacial

Aurélia Ferrari 21/3/2018 17:00
Deleted: might

Aurélia Ferrari 13/2/2018 10:31
Deleted: 8

events in the westernmost Corinth Rift during the Holocene. Bars without error bars in the second panel indicate minimum sedimentation rates.

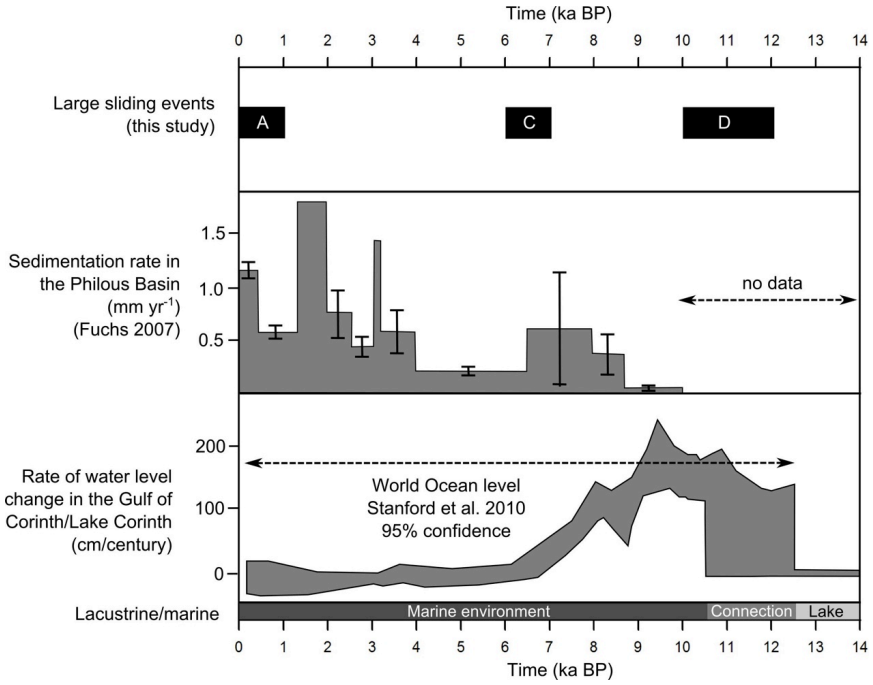

5.6 Conceptual model for the sliding events

Large sliding events (total volume $\geq 10^8$ m^3) occurred in the westernmost Gulf of Corinth with fairly long recurrence intervals, ≥ 2.5 ka. We suggest that their temporal distribution is primarily controlled by changes in pre-conditioning factors, which were a prerequisite for any landslide trigger to be effective. In other words, the clustering of slope failures during distinct sliding events would depend on the appropriate state of pre-conditioning factors, which occur only during limited periods of time. Two types of pre-conditioning factors would have played a significant role, on one hand increased denudation rates, identified at 17-70 ka, 6.5-8.5 ka and 0-4 ka and, on the other hand, dramatic changes in oceanographic conditions that occurred at 10-12 ka. More generally, the SE frequency would reflect the time needed to reload submarine slopes beyond their stability threshold after each event. Once the pre-conditioning factor evolution has made the slopes prone to sliding, each individual sliding event is characterized by either simultaneous submarine landslides producing large coalesced MTDs and pointing to a likely seismic trigger (SEs C, D and F) or separate smaller slides caused by various lower-intensity triggers (earthquakes, exceptional onshore flood events, as exemplified by the 1995 and 1963 coastal landslides, respectively) over a few centuries (SE A).

Aurélia Ferrari 21/3/2018 22:11
Deleted: may

Finally, we underline that the sliding processes have not been clearly identified in this study. Lykousis et al. (2009) mention debris flows and avalanches for slope failures on steep fan-delta slopes (2-6°) in the western Gulf of Corinth, and rotational slumps on low angle (0.5-2°) prodelta slopes. One sharp head scarp identified in this study also shows that at least one translational slide happened in hemipelagites accumulated far from the main river outlets.

5.7 Implications for tsunami hazard in the Gulf of Corinth

Among the 32 MTDs identified in this study, MTD 19 stands out as a particularly large feature (a little less than 1 km^3 in volume). This is 6 times the volume of the second largest MDT identified in this study, and about two orders of magnitude larger than the range previously proposed for the size of submarine landslides in the westernmost Gulf of Corinth (Lykousis et al., 2007). It is also 6 times larger than the largest MTD reported in the rest of the Gulf of Corinth, which occurred in the area of the Perachora Peninsula (Papatheodorou et al.,1993; Stefatos et al., 2006). MTD 19 likely resulted from the coalescence of at least two probably synchronous major slides. If correct, these slides should have triggered very large tsunamis waves, probably larger than those reported by historical sources in the westernmost Gulf of Corinth, which were triggered by small to medium-sized slope failures (Papadopoulos 2003; Stefatos et al., 2006; Tinti et al., 2007).

6 Conclusion

We documented the existence of large mass wasting events during the Holocene and the Late Pleistocene in the westernmost Gulf of Corinth. Mass wasting events consist in submarine or coastal landslides that occurred during short periods of time. Six large mass wasting events are listed, their associated deposits locally representing 30% of the sedimentation since 130 ka in the Delphic Plateau Basin. In the case of large MTDs (up to almost 1 km^3 for the largest), a simultaneous triggering of separate slope failures is proposed, suggesting a seismic origin. However, it is suggested that the temporal distribution of sliding events is primarily controlled by the evolution of pre-conditioning factors. Two main pre-conditioning factors are identified, namely (1) the time needed to slope reloading after an event, which varied in relation with temporally varying sedimentation rates, and (2) dramatic changes in water depth and water circulation that occurred 10-12 ka ago during the last post-glacial transgression. Finally, it is likely that these sliding events have triggered large tsunami waves in the whole Gulf of Corinth, in some cases (much?) larger than those reported in historical sources.

Competing interests. The authors declare they have no conflict of interest.

Acknowledgement. This work has been funded within the ANR SISCOR project directed by Pascal Bernard, at Institut de Physique du Globe (Paris) and by FNRS- Grant for Researchers (CC) ID 14633841. Arnaud Beckers's PhD grant was supported by the Belgian FRIA. Funding for Arnaud Beckers' stays in the ISTerre Laboratory was provided by a grant from la Région Rhône-Alpes. The authors warmly acknowledge R/V ALKYON's crew, Koen De Rycker (RCMG), and Pascale Bascou (ISTerre) for technical support, and the whole SISCOR scientific team for fruitful discussions.

References

Beck, C., Mercier de Lépinay, B., Schneider, J.-L., Cremer, M., Cagatay, N., Wendenbaum, E., Boutareaud, S., Ménot, G., Schmidt, S., Weber, O., Eris, K., Armijo, R., Meyer, B., & Pondard, N. (2007). Late Quaternary co-seismic sedimentation in the Sea of Marmara's deep basins. Sedimentary Geology, 199 (1-2), 65-89.

Beckers, A., Hubert-Ferrari, A., Beck, C., Bodeux, S., Tripsanas, E., Sakellariou, D., & De Batist, M. (2015). Active faulting at the western tip of the Gulf of Corinth, Greece, from high-resolution seismic data. Marine Geology, 360, 55-69.

Beckers, A., 2015, Late quaternary sedimentation in the western gulf of Corinth : interplay between tectonic deformation, seismicity, and eustatic changes, PhD thesis, pp. 260.

Beckers, A., Beck, C., Hubert-Ferrari, A., Tripsanas, E., Crouzet, C., Sakellariou, D., Papatheodorou, G. & De Batist, M. (2016). Influence of bottom currents on the sedimentary processes at the western tip of the Gulf of Corinth, Greece. Marine Geology, 378, 312-332.

779 Beckers, A., Beck, C., Hubert-Ferrari, A., Reyss, J. L., Mortier, C., Albini, P., Rovida, A., Develle, A.-
780 L., Tripsanas, E., Sakellariou, D., Crouzet, C. & Scotti, O. (2017). Sedimentary impacts of recent
781 moderate earthquakes from the shelves to the basin floor in the western Gulf of Corinth. Marine
782 Geology, 384, 81-102.
783
784 Briole, P., Rigo, A., Lyon-Caen, H., Ruegg, J., Papazissi, K., Mitsakaki, C., Balodimou A., Veis G.,
785 Hatzfeld F., and Deschamps A. (2000). Active deformation of the Corinth rift, Greece: Results from
786 repetead Global Positioning System surveys between 1990 and 1995. Journal of geophysical research,
787 105 (B11), 25605-25625.
788
789 Campos, C., Beck, C., Crouzet, C., Carrillo, E., Welden, A. V., & Tripsanas, E. (2013). Late Quaternary
790 paleoseismic sedimentary archive from deep central Gulf of Corinth : time distribution of inferred
791 earthquake-induced layer. Annals of Geophysics, 56 (6), 1-15.
792
793 Collier, R. E., Leeder, M. R., Trout, M., Ferentinos, G., Lyberis, E., & Papatheodorou, G. (2000). High
794 sediment yields and cool, wet winters: Test of last glacial paleoclimates in the northern Mediterranean.
795 Geology, 28, 999-1002.
796
797 Cotterill, C. (2006). A High-resolution Holocene Fault Activity History of the Aigion Shelf, Gulf of
798 Corinth, Greece. PhD thesis, PhD Thesis, University of Southampton.
799
800 De Martini, P., Pavlopoulos, K., Pantosti, D., & Palyvos, N. (2007). 3HAZ Corinth Deliverable 73:
801 Dating of paleo-tsunamis. Tech. rep., Istituto Nazionale di Geofisica e Vulcanologia, Roma.
802
803 Demoulin, A., Beckers, A. & Hubert-Ferrari, A. (2015). Patterns of Quaternary uplift of the Corinth rift
804 southern border (N Peloponnese, Greece) revealed by fluvial landscape morphometry. Geomorphology
805 246, 188–204. doi:10.1016/j.geomorph.2015.05.032.
806
807 Ferentinos, G., Papatheodorou, G., & Collins, M. (1988). Sediment Transport processes on an active
808 submarine fault escarpment: Gulf of Corinth, Greece. Marine Geology, 83 (1-4), 43-61.
809
810 Fuchs, M. (2007). An assessment of human versus climatic impacts on Holocene soil erosion in NE
811 Peloponnese, Greece. Quaternary Research, 67 (3), 349-356.
812
813 Galanopoulos, A., Delimbasis, N., & Comninakis, P. (1964). A tsunami generated by a slide without a
814 seismic shock. Geological Chronicles of Greece, 16, 93-110.
815
816 Hasiotis, T., Charalampakis, M., Stefatos, a., Papatheodorou, G. & Ferentinos, G. (2006). Fan delta de-
817 velopment and processes offshore a seasonal river in a seismically active region, NW Gulf of Corinth.
818 Geo-Marine Letters, 26, 199–211. doi:10.1007/s00367-006-0020-8.
819
820
821 Heezen, B. C., Ewing, M., & Johnson, G. L. (1966). The Gulf of Corinth floor. Deep-Sea research, 13,
822 381-411.
823
824 Kontopoulos, N., & Avramidis, P. (2003). A late Holocene record of environmental changes from the
825 Aliki lagoon, Egion, North Peloponnesus, Greece. Quaternary International, 111 (1), 75-90.
826
827 Koukouvelas, I. K., Katsonopoulou, D., Soter, S., & Xypolias, P. (2005). Slip rates on the Helike Fault,
828 Gulf of Corinth, Greece: New evidence from geoarchaeology. Terra Nova, 17 (2), 158-164.
829
830 Kortekaas, S., Papadopoulos, G.A., Ganas, A., Cundy, A., & Diakantoni, A. (2011). Geological
831 identification of historical tsunamis in the Gulf of Corinth, Central Greece. Natural Hazards and Earth
832 System Science, 11 (7), 2029-2041.

Leeder, M. R., Harris, T., & Kirkby, M. J. (1998). Sediment supply and climate change: implications for basin stratigraphy. Basin Research, 10 , 7-18.

Lorito, S., Tiberti, M. M., Basili, R., Piatanesi, A., & Valensise, G. (2008). Earthquake-generated tsunamis in the Mediterranean Sea: Scenarios of potential threats to Southern Italy. Journal of Geophysical Research, 113 (B1), B01301.

Lykousis, V., Sakellariou, D., Rousakis, G., Alexandri, S., Kaberi, H., Nomikou, P., Georgiou P. & Balas, D. (2007). Sediment failure processes in active grabens: the western gulf of Corinth (greece). in V. Lykousis, D. Sakellariou, & J. Locat (Éds.), Submarine Mass Movements and their Consequences III (pp. 297-305). Springer.

Lykousis, V., Roussakis, G., & Sakellariou, D. (2009). Slope failures and stability analysis of shallow water prodeltas in the active margins of Western Greece, northeastern Mediterranean Se. International Journal of Earth Sciences, 98 (4), 807-822.

McNeill, L., Cotterill, C., Henstock, T., Bull, J., Stefatos, A., Collier, R., Papatheoderou, G., Ferentinos, G., & Hick S.E. (2005). Active faulting within the offshore western Gulf of Corinth, Greece: Implications for models of continental rift deformation. Geology, 33 (4), 241.

Moernaut, J., De Batist, M., Charlet, F., Heirman, K., Chapron, E., Pino, M., Brümmer, R. & Urrutia, R. (2007). Giant earthquakes in South-Central Chile revealed by Holocene mass-wasting events in Lake Puyehue. Sedimentary Geology 195, 239–256. doi:10.1016/j.sedgeo.2006.08.005.

Moernaut, J., De Batist, M., Heirman, K., Van Daele, M., Pino, M., Brümmer, R., & Urrutia, R. (2009). Fluidization of buried mass-wasting deposits in lake sediments and its relevance for paleoseismology: Results from a reflection seismic study of lakes Villarrica and Calafquen (South-Central Chile). Sedimentary Geology, 213 (3-4), 121-135.

Moernaut, J., & De Batist, M. (2011). Frontal emplacement and mobility of sublacustrine landslides: Results from morphometric and seismostratigraphic analysis. Marine Geology 285 (2011) 29–45, doi:10.1016/j.margeo.2011.05.001

Moernaut, J., Van Daele, M., Strasser, M., & De Batist, M. (2015). A lacustrine perspective on turbidite and landslide cycles : implications for subaquatic paleoseismology. Turbidites: process and records, in: Oral communication at the ISC 2015, Geneva.

Moretti, I., Lykousis, V., Sakellariou, D., Reynaud, J.-Y., Benziane, B., & Prinzhoffer, A. (2004). Sedimentation and subsidence rate in the Gulf of Corinth: what we learn from the Marion Dufresne's long-piston coring. Comptes Rendus Geoscience, 336 (4-5), 291-299.

Nomikou, P., Alexandri, M., Lykousis, V., Sakellariou, D., & Ballas, D. (2011, September). Swath bathymetry and morphological slope analysis of the Corinth Gulf. In Grützner C. Pérez-López R. Fernandez Steeger T. Papanikolaou I. Reicherter K. Silva PG & Vött A.(eds) Earthquake Geology and Archaeology: Science, Society and Critical Facilities. 2nd INQUA-IGCP-567 International Workshop on Active Tectonics, Earthquake Geology, Archeology and Engineering, 19-24.

Pantosti, D., De Martini, P. M., Koukouvelas, I., Stamatopoulos, L., Palyvos, N., Pucci, S., Lemielle, F., & Pavlides, S. (2004). Palaeoseismological investigations of the Aigion Fault (Gulf of Corinth, Greece). Comptes Rendus Geoscience , 336 (4-5), 335-342.

Papadopoulos, G. A. (2003). Tsunami Hazard in the Eastern Mediterranean : Strong Earthquakes and Tsunamis in the Corinth Gulf , Central Greece. Natural Hazards, 29, 437-464.

Aurélia Ferrari 21/3/2018 17:01
Deleted: .

Papatheodorou, G., & Ferentinos, G. (1993). Sedimentation processes and basin-filling depositional architecture in an active asymmetric graben: Strava graben, Gulf of Corinth, Greece. Basin Research 5, 235–253. doi:10.1111/j.1365-2117.1993.tb00069.x.

Papatheodorou, G., & Ferentinos, G. (1997). Submarine and coastal sediment failure triggered by the 1995, M = 6.1 R Aegion earthquake, Gulf of Corinth , Greece. Marine Geology, 137, 287-304.

Papathoma, M., & Dominey-Howes, D. (2003). Tsunami vulnerability assessment and its implications for coastal hazard analysis and disaster management planning, Gulf of Corinth, Greece. Natural Hazards and Earth System Science, 3 (6), 733-747.

Perissoratis, C., Piper, D. J., & Lykousis, V. (2000). Alternating marine and lacustrine sedimentation during late Quaternary in the Gulf of Corinth rift basin, central Greece. Marine geology, 167, 391-411.

Salamon, A., Rockwell, T., Ward, S. N., Guidoboni, E., & Comastri, A. (2007). Tsunami Hazard Evaluation of the Eastern Mediterranean: Historical Analysis and Selected Modeling. Bulletin of the Seismological Society of America, 97 (3), 705-724.

Soloviev, S. L. (1990). Tsunamigenic zones in the Mediterranean Sea. Natural Hazards, 3 (2), 183-202.

Stefatos, A., Charalambakis, M., Papatheodorou, G., & Ferentinos, G. (2006). Tsunamigenic sources in an active European half-graben (Gulf of Corinth, Central Greece). Marine Geology, 232 (1-2), 35-47.

Strasser, M., Anselmetti, F. S., Fah, D., Giardini, D., & Schnellmann, M. (2006). Magnitudes and source areas of large prehistoric northern Alpine earthquakes revealed by slope failures in lakes. Geology, 34 (12), 1005.

Strasser, M., Monecke, K., Schnellmann, M., & Anselmetti, F.S. (2013). Lake sediments as natural seismographs: A compiled record of Late Quaternary earthquakes in Central Switzerland and its implication for Alpine deformation. Sedimentology, 60, 319–341. doi:10.1111/sed.12003.

Taylor, B., Weiss, J. R., Goodliffe, A. M., Sachpazi, M., Laigle, M., & Hirn, A. (2011). The structures, stratigraphy and evolution of the Gulf of Corinth rift, Greece. Geophysical Journal International, 185, 1189-1219.

Tinti, S., Zaniboni, F., Armigliato, A., Pagnoni, G., Gallazzi, S., Manucci, A., Brizuela Reyes B., Bressan L., &Tonini, R., (2007). Tsunamigenic landslides in the western Corinth Gulf: numerical scenarios. In V. Lykousis, & D. Sakellariou (Éds.), Submarine Mass Movements and their Consequences (pp. 405-414). Springer.

Tripsanas, E. K. & Piper, D.J.W. (2008). Glaciogenic Debris-Flow Deposits of Orphan Basin, Offshore Eastern Canada: Sedimentological and Rheological Properties, Origin, and Relationship to Meltwater Discharge. Journal of Sedimentary Research, 78, 724-744.

Urlaub, M., Talling, P.J., & Masson, D.G. (2013). Timing and frequency of large submarine landslides: Impli- cations for understanding triggers and future geohazard. Quaternary Science Reviews, 72, 63–82. URL: Link, doi:10.1016/j.quascirev.2013.04.020.

Van Welden, A. (2007). Enregistrements sédimentaires imbriqués d'une activité sismique et de changements paléo-environnementaux. Etude comparée de différents sites: Golfe de Corinthe (Grèce), Lac de Shkodra (Alabanie/Montenegro), Golfe de Cariaco (Vénézuela). PhD thesis, University of Savoie

Woessner, J., Giardini, D., & Danciu, L. (2013). SHARE project, D5.“ Final seismic hazard assessment including aggregation. Tech. rep., Swiss Seismological Service.

Zitter, T.A.C., Grall, C., Henry, P., Ozeren, M.S., Cagatay, M.N., Sengor, A.M.C., Gasperini, L., de Lépinay, B.M., & Géli, L. (2012). Distribution, morphology and triggers of submarine mass wasting in the Sea of Marmara. Marine Geology 329-331, 58–74. doi:10.1016/j.margeo.2012.09.002.

Page 13: [1] Deleted Aurélia Ferrari 21/02/2018 14:31

Right: Spatial extent and thickness of the largest MTD from the presented inventory (MTD 19, sliding event F). Contours represent the sea floor bathymetry (one line every 20 m).